

# SYMMETRIC CONFIGURATION SPACES OF LINKAGES

DAVID BLANC AND NIR SHVALB

ABSTRACT. A *configuration* of a linkage  $\Gamma$  is a possible positioning of  $\Gamma$  in  $\mathbb{R}^d$ , and the collection of all such forms the configuration space  $\mathcal{C}(\Gamma)$  of  $\Gamma$ . We here introduce the notion of the *symmetric configuration space* of a linkage, in which we identify configurations which are geometrically indistinguishable. We show that the symmetric configuration space of a planar polygon has a regular cell structure, provide some principles for calculating this structure, and give a complete description of the symmetric configuration space of all quadrilaterals and of the equilateral pentagon.

## 1. Introduction

The mathematical theory of robotics is based on the notion of a mechanism consisting of links connected by flexible joints. More precisely, a *linkage*  $\Gamma$  is a metric graph, with edges (of fixed lengths) corresponding to the links, and vertices corresponding to the joints. See [Me,S,T] and [F2] for surveys of the mechanical and topological aspects, respectively.

A central tool in studying such a linkage is its configuration space  $\mathcal{C}(\Gamma)$ , a topological space whose points correspond to possible positionings of  $\Gamma$  in the ambient Euclidean space  $\mathbb{R}^d$ . These spaces are useful for understanding actuations, motion planning, and singular configurations of the mechanisms (see, e.g., [FG,KTe,KTs,MT,SSBB,SSB]); in recent years, the related notion of topological complexity has been a topic of much research (see [F1] and [BGRT, BR,BK,C,D,FP,MW]).

Observe that in the standard construction of  $\mathcal{C}(\Gamma)$  we distinguish between configurations which are functionally equivalent though formally distinct: thus if  $\Gamma$  consists of a fixed platform with two identical free arms  $ABC$  and  $ADE$ , the two positions shown in Figure 1 are considered distinct configurations, but are functionally the same. Thus it makes sense to consider a version of the configuration space in which they are identified.

For this purpose, we introduce the notion of the *symmetric configuration space* of a linkage  $\Gamma$ , in which points of the usual configuration space  $\mathcal{C}(\Gamma)$  are identified if they differ by an automorphism of  $\Gamma$  – which we can think of

---

2020 *Mathematics Subject Classification*. Primary 70G40; Secondary 57R45, 70B15.

*Key words and phrases*. configuration space, workspace, robotics, mechanism, linkage, kinematic, symmetry.

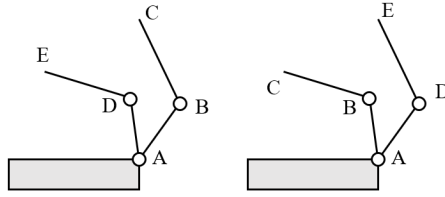


FIGURE 1. Two arm mechanism

as a relabelling of vertices of  $\Gamma$  which does not change its geometric relations (i.e., which vertices are connected by an edge, and the length of this edge). One should note that there are two useful versions of the configuration space of a linkage, *fully reduced* and *reduced* (depending on whether we divide the set of embeddings by all Euclidean isometries of the ambient space  $\mathbb{R}^d$ , or only by the orientation-preserving ones – see §2.1 below). There are also two corresponding types of symmetric configuration spaces.

Although to the best of our knowledge, the concept of the symmetric configuration space of a linkage has not appeared in the mathematical or engineering literature, it has an obvious intuitive meaning: in real life, mechanisms do not have natural labellings of their joints, and for practical purposes, the two arms of Figure 1 are indistinguishable. Of course, if each arm is used to grasp a different object, the distinction is important, which is why the usual notion of a configuration space is more generally applicable. However, for motion planning for the two-arm mechanism from rest, the symmetric configuration space is the more economical version to use.

Intuitively, each point in the symmetric configuration space can be thought of as instructions for specifying a rigid configuration of a real-life linkage in the ambient space  $\mathbb{R}^d$  ( $d = 2, 3$ ), without labelling links or joints which are indistinguishable in the abstract mechanism  $\Gamma$ .

Another possible application is to molecules with structural symmetries, whose reduced configuration space represents the mutual positions of their constituent atoms in space (the fully reduced configuration space does not distinguish between the two chiralities, if they exist). See, e.g., [HS, Ch. III].

Our main results in this paper are concerned with the planar configurations of the closed chain with  $n$  links. On a theoretical level, we provide a systematic approach to describing an equivariant cell structure on the configuration space of a closed chain under action of the group  $\text{Aut}(\Gamma)$  of automorphisms of the linkage:

**Theorem A.** *The reduced configuration space of an  $n$ -gon in the plane has a regular  $\text{Aut}(\Gamma)$ -equivariant cell structure, subordinate to the standard regular cell structure, and similarly for the fully reduced configuration space.*

See Theorem 5.3 and Corollary 5.4 below. From the equivariant cell structure for these two types of configuration space we can then derive directly an induced (ordinary) cell structure for the two types of symmetric configuration space.

The symmetric cells of the configuration space – that is, those fixed under various subgroups of  $H \leq \text{Aut}(\Gamma)$  – play a central role in describing the cell structure of two types of symmetric configuration spaces, and we show:

**Theorem B.** *The fixed point set of the fully reduced configuration space of a planar polygon  $\Gamma$  under a subgroup  $H$  of  $\text{Aut}(\Gamma)$  is a disjoint union of components (indexed by the discrete set of configurations fixed under  $\text{Aut}(\Gamma)$  itself), each of which fibers successively over intervals or tori.*

See Propositions 6.1 and 6.4 and Theorem 6.8 for a more precise description.

The remainder of the paper is devoted to two specific calculations. We show:

**Theorem C.** *The reduced symmetric configuration space of a planar quadrilateral is homeomorphic to a closed interval, a circle, a wedge of a circle and a segment, or a circle with its diameter.*

See Theorem 3.3 below, where the cases in which each value obtains are described in full.

**Proposition D.** *The fully reduced symmetric configuration space of the planar equilateral pentagon is homeomorphic to a closed disc.*

See Proposition 8.1 below.

## 1.1. Organization and main results

In Section 2 we review the main notions needed to define the various types of configuration spaces of a mechanism, and introduce the corresponding versions of symmetric configuration spaces. Simple examples of symmetric configuration spaces are given in Section 3, including a full description of planar quadrilaterals (with the details appearing in Appendix A). In Section 4 we recall some general facts about the configuration spaces of planar polygons in general, including their cell structure. Section 5 is devoted to the automorphisms of planar polygons  $\Gamma$ , culminating in Theorem 5.3. Section 6 discusses symmetric configurations for planar polygons – that is, the fixed-point sets of the configuration space under various subgroups  $H$  of  $\text{Aut}(\Gamma)$ . Section 7 shows how these general results may be applied to obtain an equivariant triangulation of one non-equivariant cell, in the case where  $\Gamma$  is the equilateral hexagon. Finally, Section 8 provides a full description of the fully reduced symmetric configuration space of the equilateral pentagon.

## 2. Configuration spaces

We first recall some general background material on the construction and basic properties of configuration spaces. This also serves to fix notation, which is not always consistent in the literature.

**Definition.** Consider an abstract graph  $\mathcal{T}^\Gamma$  with vertices  $V$  and edges  $E \subseteq V^2$  (with no loops or parallel edges, but not necessarily connected). A *linkage* (or *mechanism*)  $\Gamma$  of type  $\mathcal{T}^\Gamma$  is determined by a function  $\ell : E \rightarrow \mathbb{R}_+$  specifying the length  $\ell_i$  of each edge  $e_i$  in  $E = \{e_i = (u_i, v_i)\}_{i=1}^k$  (subject to the triangle inequality as needed). We write  $\vec{\ell} := (\ell_1, \dots, \ell_k) \in \mathbb{R}^E$  for the vector of lengths.

The *configuration space* of the linkage  $\Gamma$  is the metric subspace  $\mathcal{C}(\Gamma) := \lambda^{-1}(\vec{\ell})$  of  $(\mathbb{R}^d)^V$  (a real algebraic variety), where the map  $\lambda : (\mathbb{R}^d)^V \rightarrow \mathbb{R}^E$  is given by  $\lambda(u_i, v_i) := \|\varphi(u_i) - \varphi(v_i)\|$ . A point  $\mathbf{x} \in \mathcal{C}(\Gamma)$  is called a *configuration* of  $\Gamma$ . Note that  $\mathcal{C}(\Gamma)$  is a subspace of the space  $\text{Emb}^d(\mathcal{T}^\Gamma) \subseteq (\mathbb{R}^d)^V$  of *embeddings* of  $V$  in  $\mathbb{R}^d$  (without collisions).

## 2.1. Isometries of configuration spaces

The group  $\text{Euc}^d$  of isometries of the Euclidean space  $\mathbb{R}^d$  acts on the space  $\mathcal{C}(\Gamma)$ . Taking this action into account allows us to reduce the dimension of  $\mathcal{C}(\Gamma)$  without losing any interesting information, as follows:

If we choose a fixed vertex  $v_0$  of  $\Gamma$  as its *base-point*, the action of the translation subgroup  $T \cong \mathbb{R}^d$  of  $\text{Euc}^d$  on  $\mathbf{x}(v_0)$  is free, so its action on  $\mathcal{C}(\Gamma)$  is free, too, and we might reduce the degrees of freedom of  $\mathcal{C}(\Gamma)$  by considering its quotient under this action.

However, such a choice will not fit in with our notion of symmetries, so for our purposes it is more convenient to think of the coordinate frame with the barycenter  $B(\mathbf{x})$  of a given configuration  $\mathbf{x} \in \mathcal{C}(\Gamma)$  at the origin. We therefore define the *pointed configuration space* for  $\Gamma$  to be the quotient space  $\mathcal{C}_*(\Gamma) := \mathcal{C}(\Gamma)/T$  under translations. Thus  $\mathcal{C}(\Gamma) \cong \mathcal{C}_*(\Gamma) \times \mathbb{R}^d$ , and a pointed configuration (i.e., an element of  $\mathcal{C}_*(\Gamma)$ ) is simply an ordinary configuration expressed in terms of a coordinate frame for  $\mathbb{R}^d$  with the barycenter at the origin. Essentially, this means replacing the Euclidean ambient space  $\mathbb{R}^d$  by the corresponding affine space, equipped with a chosen direction for each axis.

If we divide  $\mathcal{C}(\Gamma)$  by the action of the group  $\text{Euc}_+^d$  of orientation-preserving isometries of the ambient space  $\mathbb{R}^d$ , we obtain the *reduced configuration space* of  $\Gamma$ , denoted by  $\widehat{\mathcal{C}}(\Gamma)$ . When  $\Gamma$  has a rigid “base platform”  $P$  of dimension  $\geq d-1$ , the action of  $\text{Euc}_+^d$  is free. For example, if  $d=2$ , we may fix a vertex  $v_0$  and a link  $\vec{v}$  in  $\Gamma$  starting at  $v_0$ , and let  $p : \mathcal{C}_*(\Gamma) \rightarrow S^{d-1}$  assign to a configuration  $\mathcal{V}$  the direction of  $\vec{v}$ . The fiber of  $p$   $\vec{e}_1 \in S^{d-1}$  is  $\widehat{\mathcal{C}}(\Gamma)$ .

Dividing  $\mathcal{C}(\Gamma)$  by the full group  $\text{Euc}^d$  of all isometries of  $\mathbb{R}^d$  we obtain the *fully reduced configuration space*  $\widetilde{\mathcal{C}}(\Gamma)$  of  $\Gamma$ . Note that any configuration whose image is contained in a line is fixed under reflections in that line, so the action of  $\text{Euc}^d$  may not be free. Thus  $\mathcal{C}(\Gamma)$  is not generally isomorphic to  $\widetilde{\mathcal{C}}(\Gamma) \times \text{Euc}^d$ . Nevertheless,  $\widetilde{\mathcal{C}}(\Gamma)$  is the most economical model for most linkages  $\Gamma$ .

## 2.2. Normalization

Note that the image of a configuration  $\mathbf{x} \in \mathcal{C}(\Gamma)$  is the same as the image of  $\mathbf{x} \circ f$  for any automorphism  $f : V \rightarrow V$  of the linkage  $\Gamma$  (that is, a relabelling of the vertices preserving adjacency and edge length). This does not mean that we have an isometry of  $\mathbb{R}^d$  taking  $\mathbf{x}$  to  $\mathbf{y} := \mathbf{x} \circ f$  – e.g., when  $\mathcal{T}^\Gamma$  is a bouquet of circles (closed chains), we may reflect one of them, leaving the rest in place (see also Figure 1).

However, when  $\Gamma$  has a rigid “base platform”  $P$  of dimension  $\geq d - 1$ , as above, we can identify  $\mathcal{C}(\Gamma)$  with  $\widehat{\mathcal{C}}(\Gamma) \times \text{Euc}_+^d$ : that is, every configuration  $\mathbf{x}$  in  $\mathcal{C}(\Gamma)$  can be *normalized* uniquely to a reduced configuration  $\hat{\mathbf{x}} \in \widehat{\mathcal{C}}(\Gamma)$ , by placing the platform in a standard direction and moving the barycenter of  $\mathbf{x}$  to the origin. This will be denoted by  $\hat{\mathbf{x}} = N(\mathbf{x}) = T_{\mathbf{x}}(\mathbf{x})$ , where the specific transformation  $T_{\mathbf{x}} \in \text{Euc}_+^d$  used to normalize  $\mathbf{x}$  may not depend continuously on  $\mathbf{x}$ , but  $N : \mathcal{C}(\Gamma) \rightarrow \widehat{\mathcal{C}}(\Gamma)$  is continuous, thus providing a canonical section for the quotient map  $q : \widehat{\mathcal{C}}(\Gamma) \rightarrow \mathcal{C}(\Gamma)$ .

Any polygon  $\Gamma$  in the plane always has such a rigid platform, so when  $\Gamma$  is equilateral, a reduced configuration  $\hat{\mathbf{x}}$  is completely determined by the orientation (that is, a cyclic ordering of the vertices  $A_1, \dots, A_n, A_1$ ) and the sequence of angles  $(\phi_1, \dots, \phi_n)$  at each vertex  $A_i$ , measured counter clockwise from  $\overrightarrow{A_i A_{i+1}}$  to  $\overrightarrow{A_i A_{i-1}}$ . The automorphism  $f$  is simply a permutation  $\sigma$  on  $\{1, \dots, n\}$  preserving adjacency – that is, a cyclic shift, with or without a reverse of orientation. If the orientation is preserved,  $N(\phi_1, \dots, \phi_n) = (\phi_{\sigma^{-1}(1)}, \dots, \phi_{\sigma^{-1}(n)})$ , while if  $\sigma$  reverses orientation, then  $N(\phi_1, \dots, \phi_n) = (-\phi_{\sigma^{-1}(1)}, \dots, -\phi_{\sigma^{-1}(n)})$ , since the angles should now be measured in the reverse direction.

**Example 2.1.** When  $\Gamma = \Gamma_k^{\text{op}}$  is an open chain of length  $k$  (see Figure 4 below),  $\widehat{\mathcal{C}}(\Gamma) \cong (S^{d-1})^{k-1}$ . If  $d = 2$ ,  $\widehat{\mathcal{C}}(\Gamma_k^{\text{op}})$  is a  $(k-1)$ -torus, parameterized by  $(\theta_1, \dots, \theta_{k-1})$ . The fully reduced configuration space  $\widetilde{\mathcal{C}}(\Gamma_k^{\text{op}})$  may be identified with a subspace of  $\widehat{\mathcal{C}}(\Gamma_k^{\text{op}})$  defined as follows:

For  $k = 2$ ,  $\widetilde{\mathcal{C}}(\Gamma_2^{\text{op}}) = [0, \pi] \subseteq S^1$ , and we write  $\widetilde{\mathcal{C}}(\Gamma_2^{\text{op}})' = [\pi, 2\pi]$  for the version of the fully reduced configuration space in which we require the first edge not on the  $x$ -axis to point downwards.

We may then define  $\widetilde{\mathcal{C}}(\Gamma_k^{\text{op}})$  by induction on  $k \geq 2$  to be the subspace of  $(S^1)^{k-1}$  given by:

$$(0, \pi) \times (S^1)^{k-2} \cup \{0\} \times \widetilde{\mathcal{C}}(\Gamma_{k-1}^{\text{op}}) \cup \{\pi\} \times \widetilde{\mathcal{C}}(\Gamma_{k-1}^{\text{op}})'$$

Thus for  $k = 3$  we obtain a cylinder with each boundary component omitting half a circle (opposite halves at either end).

*Remark 2.2.* The configuration spaces studied in this paper are mathematical models, which take into account only the locations of the vertices of  $\Gamma$ , disregarding possible intersections of the edges. In the plane, there is some

justification for this, since we can allow one link to slide over another. This is why this model is commonly used (cf. [KM, F2]; but see [CDR]). However, in  $\mathbb{R}^3$  the model is not very realistic, since it disregards the fact that rigid rods cannot pass through each other.

Note that  $\text{Emb}^3(\mathcal{T}^\Gamma)$  has a dense open subspace  $U(\mathcal{T}^\Gamma)$  consisting of those embeddings of  $V$  which induce an embedding of the full graph (including its edges). Similarly,  $\mathcal{C}(\Gamma)$  has a dense open subspace  $U(\Gamma) := \text{Emb}^3(\mathcal{T}^\Gamma) \cap U(\mathcal{T}^\Gamma)$ . In a more realistic treatment of all configurations of  $\Gamma$  in  $\mathbb{R}^3$ , we must cut open  $\mathcal{C}(\Gamma)$  along the complement  $\mathcal{C}(\Gamma) \setminus U(\Gamma)$ , consisting of configurations with collisions. The precise description of a “realistic” configuration space  $\text{Conf}(\mathcal{T}^\Gamma)$  is quite complicated, even at the combinatorial level, which is why we work here with  $\text{Emb}^d(\mathcal{T}^\Gamma)$ ,  $\mathcal{C}(\Gamma)$ , and  $\mathcal{C}_*(\Gamma)$  as defined in §2-2.1. We observe that even such a model  $\text{Conf}(\mathcal{T}^\Gamma)$  is not completely realistic, in that it disregards the thickness of the rigid rods. See [BS2] for a fuller treatment of this issue.

### 2.3. Symmetric configurations

When a mechanism  $\Gamma$  has internal symmetries, the various flavors of configuration spaces described above may be unnecessarily complicated: if we take into account the labelling of the vertices, the two configurations in Figure 1 are not equivalent even in the fully reduced configuration space for such a linkage, though they may be the same from a practical point of view. To overcome this discrepancy, consider the following notions:

A graph  $\mathcal{T}^\Gamma$  as above has a discrete group  $\text{Aut}(\mathcal{T}^\Gamma)$  of *graph automorphisms*: the subgroup of the permutations  $f : V \rightarrow V$  on the vertex set  $V$  which preserve the (undirected) edge relation. A mechanism  $\Gamma$  with length function  $\ell : E \rightarrow \mathbb{R}_+$  has a *linkage automorphism* group  $\text{Aut}(\Gamma) \subseteq \text{Aut}(\mathcal{T}^\Gamma)$ , consisting of those graph automorphisms  $f : V \rightarrow V$  which preserve lengths. The group  $\text{Aut}(\Gamma)$  naturally acts on  $\mathcal{C}(\Gamma)$  on the right by precomposition:  $\mathbf{x} \mapsto \mathbf{x} \circ f$  (this means that we are simply *relabelling* the vertices of the given geometric configuration  $\mathbf{x}$ ), and the quotient space  $\mathcal{SC}(\Gamma) := \mathcal{C}(\Gamma) / \text{Aut}(\Gamma)$  is called the *full symmetric configuration space* of  $\Gamma$ . This action is not generally free.

Since the action of  $\text{Aut}(\Gamma)$  preserves the barycenter  $B(\mathbf{x})$  of the configuration, we define the *pointed symmetric configuration space* of  $\Gamma$  to be the subspace  $\mathcal{SC}_*(\Gamma)$  of  $\mathcal{SC}(\Gamma)$  consisting of those equivalence classes  $[\mathbf{x}]$  with  $B(\mathbf{x})$  at the origin.

However, translating by  $B(\mathbf{x})$  yields a canonical isomorphism

$$(1) \quad \mathcal{SC}_*(\Gamma) \cong \mathcal{C}_*(\Gamma) / \text{Aut}(\Gamma) := \text{Aut}(\Gamma)^{\text{op}} \backslash \mathcal{C}(\Gamma) / \mathbb{R}^d .$$

(since the two actions commute). This suggests two further definitions:

The *reduced symmetric configuration space* of  $\Gamma$  is the quotient

$$(2) \quad \widehat{\mathcal{SC}}(\Gamma) := \widehat{\mathcal{C}}(\Gamma) / \text{Aut}(\Gamma) := \text{Aut}(\Gamma)^{\text{op}} \backslash \mathcal{C}(\Gamma) / \text{Euc}_+^d \cong \text{Aut}(\Gamma)^{\text{op}} \backslash \mathcal{C}_*(\Gamma) / \text{SO}(d) ,$$

while the *fully reduced symmetric configuration space* of  $\Gamma$  is defined to be

$$(3) \quad \widehat{\mathcal{SC}}(\Gamma) := \widetilde{\mathcal{C}}(\Gamma) / \text{Aut}(\Gamma) := \text{Aut}(\Gamma)^{\text{op}} \backslash \mathcal{C}(\Gamma) / \text{Euc}^d \cong \text{Aut}(\Gamma)^{\text{op}} \backslash \mathcal{C}_*(\Gamma) / O(d),$$

Neither is canonically describable as a subspace of  $\mathcal{SC}(\Gamma)$ .

#### 2.4. Symmetries and normalization

As noted in §2.2 above, when  $\Gamma$  has a rigid base platform  $P$ , every configuration  $\mathbf{x}$  in  $\mathcal{C}(\Gamma)$  can be *normalized* to a reduced configuration  $\hat{\mathbf{x}} = N(\mathbf{x}) = T_{\mathbf{x}}(\mathbf{x})$  in  $\widehat{\mathcal{C}}(\Gamma)$ ; in particular, this is true when  $\Gamma$  is an equilateral polygon in the plane.

Under these assumptions,  $\text{Aut}(\Gamma)$  acts not only on  $\mathcal{C}(\Gamma)$ , but also on  $\widehat{\mathcal{C}}(\Gamma)$ , by sending  $\hat{\mathbf{x}}$  to  $N(\hat{\mathbf{x}} \circ f)$ , where we think of  $\widehat{\mathcal{C}}(\Gamma)$  as a subspace of  $\mathcal{C}(\Gamma)$  (but precomposition with  $f \in \text{Aut}(\Gamma)$  may take us out of  $\widehat{\mathcal{C}}(\Gamma)$ ). We then have

$$(4) \quad \mathcal{SC}(\Gamma) \cong \widehat{\mathcal{SC}}(\Gamma) \times \text{Euc}_+^d := (\widehat{\mathcal{C}}(\Gamma) / \text{Aut}(\Gamma)) \times \text{Euc}_+^d$$

(see (2)), so that

$$(5) \quad \mathcal{SC}_*(\Gamma) \cong \widehat{\mathcal{SC}}(\Gamma) \times \text{SO}(d) := (\widehat{\mathcal{C}}(\Gamma) / \text{Aut}(\Gamma)) \times \text{SO}(d).$$

(see (1)).

*Remark 2.3.* Assume that the linkage  $\Gamma$  has a rigid base platform  $P$  of dimension  $\geq d - 1$  as above. If no configuration  $\mathbf{x}$  of  $\Gamma$  has its image fully contained in an affine subspace of  $\mathbb{R}^d$  of dimension  $d - 1$ , we can always choose the normalization  $\hat{\mathbf{x}}$  of  $\mathbf{x}$  to be “positively oriented”. This means that we have a canonical section  $\widetilde{\mathcal{C}}(\Gamma) \rightarrow \mathcal{C}(\Gamma)$ , so  $\mathcal{C}(\Gamma) \cong \widetilde{\mathcal{C}}(\Gamma) \times \text{Euc}^d$  and thus  $\mathcal{SC}(\Gamma) \cong \widehat{\mathcal{SC}}(\Gamma) \times \text{Euc}^d$ .

This will happen, for instance, if  $d = 2$  and  $\Gamma = \Gamma_{2k+1}^{\text{eq}}$  is an equilateral polygon with an odd number of links.

### 3. Examples of symmetric configuration spaces

We now describe a few simple examples of symmetric configuration spaces. First, note the following:

*Remark 3.1.* When the graph  $\mathcal{T}^\Gamma$  is a chain (either open or closed), any linkage  $\Gamma$  of type  $\mathcal{T}^\Gamma$  is determined by the sequence  $\vec{\ell} := (\ell_1, \dots, \ell_k)$  of lengths of the consecutive links, and a pointed configuration  $\mathbf{x}$  for  $\Gamma$  is thus completely determined by a sequence of vectors  $(\vec{\mathbf{v}}_1, \dots, \vec{\mathbf{v}}_k)$  in  $\mathbb{R}^d$  (with  $\|\vec{\mathbf{v}}_i\| = \ell_i$  for  $i = 1, \dots, k$ ), subject to the additional constraint that  $\sum_{i=1}^k \vec{\mathbf{v}}_i = \vec{\mathbf{0}}$  in the case of a closed chain (see [F2, §1.3]).

We thus see that if we re-order the sequence  $\vec{\ell} := (\ell_1, \dots, \ell_k)$ , the new mechanism  $\Gamma'$  will have a canonically isomorphic configuration space. However, the automorphisms of  $\Gamma$  need have no direct relations with those of  $\Gamma'$ , so the resulting symmetric configuration spaces may differ.

### 3.1. Open chains

When  $\mathcal{J}^\Gamma$  is an open chain of length  $k$ , there can be at most one non-trivial automorphism of the corresponding linkage  $\Gamma$  – namely, the inversion – if  $\vec{\ell} := (\ell_1, \dots, \ell_k)$  is symmetric (i.e.,  $\ell_i = \ell_{k+1-i}$  for all  $1 \leq i \leq k$ ).

- (i) If  $k = d = 2$ , with vertices  $A, B, C$ , the reduced configuration space  $\widehat{\mathcal{C}}(\Gamma)$  is  $S^1$ , with parameter  $\alpha$  equal to the angle from  $\vec{BA}$  to  $\vec{BC}$ , taken in the positive direction (and the fully reduced configuration space  $\widetilde{\mathcal{C}}(\Gamma)$  is a half circle). The  $C_2$ -action (for symmetric  $\vec{\ell}$ ) switches  $A$  and  $C$ , and therefore takes  $\alpha$  to  $2\pi - \alpha$ . Thus we have two fixed points ( $\alpha = 0, \pi$ ), and  $\widehat{\mathcal{SC}}(\Gamma)$  is an arc (with endpoints corresponding to the two fixed points).
- (ii) If  $k = 3$  and  $d = 2$ , with vertices  $A, B, C, D$ , then  $\widehat{\mathcal{C}}(\Gamma)$  is a torus  $S^1 \times S^1$  with parameters  $\theta = \angle ABC$  and  $\phi = \angle BCD$  measured as above. For symmetric  $\vec{\ell}$ , the  $C_2$ -action takes  $(\theta, \phi)$  to  $(2\pi - \phi, 2\pi - \theta)$ , with fixed points on the anti-diagonal  $\Delta := \{(\theta, \phi) \mid \phi + \theta = 2\pi\}$ . Since the action is generated by reflection in  $\Delta$ , if we think of  $\widehat{\mathcal{C}}(\Gamma)$  as usual as a square with opposite sides identified, in  $\widehat{\mathcal{SC}}(\Gamma)$  we first reflect in  $\Delta$  to obtain a triangle  $\triangle PQR$  (with  $PR$  corresponding to  $\Delta$ ), and then identify  $PQ$  with  $QR$  to obtain a projective plane with a disc removed along  $PR$  – that is,  $\widehat{\mathcal{SC}}(\Gamma)$  is a Möbius band.
- (iii) As noted in §2.1, in general  $\widehat{\mathcal{C}}(\Gamma) \cong (S^{d-1})^{k-1}$ . When  $k = 2m + 2$  and  $d = 2$ ,  $\widehat{\mathcal{C}}(\Gamma)$  is parameterized by  $(\theta_1, \dots, \theta_m, \alpha, \phi_m, \dots, \phi_1)$ . In the symmetric case, the  $C_2$ -action sends this to  $(2\pi - \phi_1, \dots, 2\pi - \phi_m, 2\pi - \alpha, 2\pi - \theta_m, \dots, 2\pi - \theta_1)$ , so the fixed points constitute an  $m$ -dimensional subspace with  $\alpha = 0, \pi$ . When  $k$  is odd, we have no central parameter  $\alpha$ .

### 3.2. Triangles

When  $\mathcal{J}^\Gamma$  is a closed chain of length 3, there is only one embedding  $\mathbf{x}$  of any triangle  $\Gamma$  in  $\mathbb{R}^2$ , up to isometry, so  $\mathcal{C}(\Gamma) \cong \text{Euc}^2$ .

- (i) When  $\Gamma$  is scalene,  $\text{Aut}(\Gamma)$  is trivial, so  $\mathcal{SC}(\Gamma) = \mathcal{C}(\Gamma)$ .
- (ii) When  $\Gamma$  is an isosceles triangle,  $\text{Aut}(\Gamma) = C_2$ , and its action on an embedding  $\mathbf{x} : \Gamma \rightarrow \mathbb{R}^2$  is equivalent to reflection in the median, so

$$\mathcal{SC}(\Gamma) = \text{Euc}^2 / C_2 \cong \text{Euc}_+^2 = \mathbb{R}^2 \times S^1$$

and thus  $\mathcal{SC}_*(\Gamma) \cong S^1$  and  $\widehat{\mathcal{SC}}(\Gamma)$  is a single point.

- (iii) When  $\Gamma = \Gamma_3^{\text{eq}}$  is equilateral,  $\text{Aut}(\Gamma) = S_3$  is the full symmetric group, so after dividing out by the reflection we have  $\text{Aut}(\Gamma) / \{\pm 1\} = A_3$  (a cyclic group of order 3), and thus  $\mathcal{SC}(\Gamma) = \mathbb{R}^2 \times (S^1 / A_3)$ , with  $\mathcal{SC}_*(\Gamma) \cong S^1$  again.



### 3.3. Quadrilaterals

The usual configuration spaces of planar quadrilaterals are easy to analyze in terms of the length vector  $\vec{\ell} = (\ell_1, \ell_2, \ell_3, \ell_4)$ . Note that  $\vec{\ell}$  must satisfy certain inequalities in order to have a non-empty (or non-trivial) configuration space – e.g., if  $\ell_1 > \ell_2$ , we must have  $\ell_1 - \ell_2 < \ell_3 + \ell_4$  (see [F2, Lemma 1.4])

It is easy to see that  $\text{Aut}(\Gamma)$  is non-trivial exactly in the following four cases:

- (1) An equilateral quadrilateral  $\Gamma = \Gamma_4^{\text{eq}}$  with  $\ell_1 = \ell_2 = \ell_3 = \ell_4$ , – in which case  $\text{Aut}(\Gamma) = D_4$  (the dihedral group of order 8).
- (2) Two pairs of adjacent links have equal lengths:  $\ell_1 = \ell_2 > \ell_3 = \ell_4$ , – in which case  $\text{Aut}(\Gamma) = C_2$ , generated by the reflection exchanging the equal links.
- (3) Each pair of opposing links has equal lengths (distinct from each other) – in which case  $\text{Aut}(\Gamma) = C_2 \times C_2$ , generated by the two interchanges of opposites.
- (4) Two opposite links are equal (but not all four) – in which case  $\text{Aut}(\Gamma) = C_2$ , generated by the reflection exchanging the equal links.

### 3.4. Parameterizing the configuration space of a quadrilateral

When  $\Gamma = ABCD$  is a quadrilateral in the plane, for generic (non-equilateral)  $\vec{\ell}$ , any reduced configuration  $\hat{\mathbf{x}}$  of  $\Gamma$  is determined by the angle  $\phi = \angle BAD$  (measured counter clockwise from  $\vec{AD}$  to  $\vec{AB}$ ), together with the “elbow up”-“elbow down” position  $\varepsilon$  of  $BCD$  – that is, whether the  $\beta = \angle BCD$  (measured counter clockwise from  $\vec{CB}$  to  $\vec{CD}$ ) satisfies  $0 < \beta < \pi$ , in which case  $\varepsilon := +1$ , or  $\pi < \beta < 2\pi$ , in which case  $\varepsilon := -1$ . If  $\beta = 0$  or  $\alpha = \pi$ , we say  $ABC$  is *aligned* and set  $\varepsilon := 0$ . Note that this last case is completely determined by the value of  $\phi$  (but may never occur, depending on the length vector  $\vec{\ell}$ ).

In the equilateral case, when  $\phi = 0 = \alpha$  (that is, the edge  $AB$  coincides with  $AD$  and  $CB$  coincides with  $CD$ ), we need an additional parameter, namely, the angle  $\theta$  between these two collapsed intervals. This suggests that the correct way to parameterize  $\widehat{\mathcal{C}}(\Gamma)$  (for any planar  $n$ -polygon) is to embed it into the  $n$ -torus  $\mathbb{T}^n = (S^1)^n$  by keeping track of the angles (oriented as above) at *each* vertex. In this situation  $\mathcal{C}(\Gamma)$  is the subspace of  $\mathbb{T}^n$  determined by the requirement that the open chain reduced configuration  $\hat{\mathbf{x}}$  defined by any  $n - 1$  successive vertex angles close up and the new angle formed is equal to the remaining vertex angle parameter. This description is more wasteful than the above, but is better suited to discussing symmetries.

### 3.5. The reduced configuration space of a quadrilateral

By Remark 3.1, for the ordinary reduced configuration space  $\widehat{\mathcal{C}}(\Gamma)$  of a quadrilateral, we may assume  $\ell_1 \geq \ell_2 \geq \ell_3 \geq \ell_4$ .

Using the method of [MT], we have the following six cases, with the reduced configuration space  $\widehat{\mathcal{C}}(\Gamma)$  given in [F2, §1.3]:

- (i)  $\ell_2 < \ell_1 < \ell_2 + \ell_3 + \ell_4$  and  $\ell_2 + \ell_3 < \ell_1 + \ell_4$ , with  $\mathcal{C}(\Gamma) \cong S^1$ .  
Here  $\text{Aut}(\Gamma) \neq \{1\}$  if and only if  $\ell_2 = \ell_3$  or  $\ell_3 = \ell_4$  (opposing) or any linkage for which  $\ell_1 > \ell_2 = \ell_3 = \ell_4$ .
- (ii)  $\ell_2 < \ell_1 < \ell_2 + \ell_3 + \ell_4$  and  $\ell_2 + \ell_3 = \ell_1 + \ell_4$ , with  $\mathcal{C}(\Gamma) \cong S^1 \vee S^1$ .  
Here  $\text{Aut}(\Gamma) \neq \{1\}$  if and only if  $\ell_2 = \ell_3$  (opposing).
- (iii)  $\ell_1 > \ell_2$  and  $\ell_2 + \ell_3 > \ell_1 + \ell_4$ , with  $\mathcal{C}(\Gamma) \cong S^1 \amalg S^1$ .  
Again  $\text{Aut}(\Gamma) \neq \{1\}$  if and only if  $\ell_2 = \ell_3$  (opposing).
- (iv)  $\ell_1 = \ell_2 \geq \ell_3 > \ell_4$ , with  $\mathcal{C}(\Gamma) \cong S^1 \amalg S^1$ .  
Here  $\text{Aut}(\Gamma) \neq \{1\}$  if and only if  $\ell_1$  is opposite  $\ell_2$ .
- (v)  $\ell_1 = \ell_2 > \ell_3 = \ell_4$ , with  $\widehat{\mathcal{C}}(\Gamma)$  as in Figure 27.  
Here  $\text{Aut}(\Gamma) = C_2$  or  $C_2 \times C_2$  in cases (2) or (3) respectively.
- (vi)  $\ell_1 = \ell_2 = \ell_3 = \ell_4$ , with  $\mathcal{C}(\Gamma) \cong S^1 \vee S^1 \vee S^1 \vee S^1$  and  $\text{Aut}(\Gamma) = D_4$ .

**Notation 3.2.** For a quadrilateral  $\Gamma = \square ABCD$  we write  $p := AB$ ,  $q := BC$ ,  $r := CD$ , and  $s := DA$  for the four values of  $\vec{\ell}$  in order, and assume without loss of generality that  $s = \ell_1$  is the longest.

**Theorem 3.3.** *In the notation of §3.2, the symmetric configuration space  $\widetilde{\mathcal{S}\mathcal{C}}(\Gamma)$  of any quadrilateral  $\Gamma$  is:*

- (i) A closed interval, if  $s > p, q, r$ ,  $p = r$ ,  $s < p + q + r$ , and  $s + q > 2p$ ;
- (ii) A circle, if  $s > p, q, r$ ,  $p = r$ ,  $s < p + q + r$ , and  $s + q \leq 2p$ , or if  $s = q \geq p > r$ .
- (iii) A wedge of a circle and a segment, if  $s = q > p = r$  (a parallelogram).
- (iv) A circle with its diameter, if  $s = p > q = r$  (a deltoid).
- (v) A closed interval, if  $s = p = q = r$  (an equilateral quadrilateral).

Since the proof of Theorem 3.3 requires checking many special cases, it is relegated to Appendix A.

*Remark 3.4.* The fully reduced symmetric configuration space  $\widetilde{\mathcal{S}\mathcal{C}}(\Gamma)$  is generally different from  $\widehat{\mathcal{S}\mathcal{C}}(\Gamma)$ . However, for the equilateral quadrilateral  $\Gamma = \Gamma_4^{\text{eq}}$ , they are the identical, in fact. This is because the fully reduced configuration space  $\widetilde{\mathcal{C}}(\Gamma)$  is the upper half of the reduced configuration space  $\widehat{\mathcal{C}}(\Gamma)$  (see Figure 29), and  $\widetilde{\mathcal{S}\mathcal{C}}(\Gamma)$  is then obtained from  $\widetilde{\mathcal{C}}(\Gamma)$  by further identifying the right and left hand sides.

Intuitively, this is because an abstract (i.e., unlabelled) configuration for a rhombus has no distinguished orientation (unlike a scalene quadrilateral, where all four angles are generally distinct, so can be oriented in the positive direction).

#### 4. General planar polygons

When  $\mathcal{T}^\Gamma$  is a polygon with more than four edges, the analysis we made above (and in Appendix A) becomes more complicated, and the number of cases too large for a full description to be useful. However, it may still be possible to say something about the cell structure of the configuration space  $\mathcal{C}(\Gamma)$  for the various mechanisms  $\Gamma$  of type  $\mathcal{T}^\Gamma$ . Moreover, the diffeomorphism type of  $\mathcal{C}(\Gamma)$  (as a manifold with singularities) depends generically only on inequalities among sums of subsets of  $\vec{\ell}$  (see [HR, Theorem 1.1]).

In this section, we recall a classical approach to such cell structures.

##### 4.1. Arrow diagrams

The pointed configuration space  $\mathcal{C}_*(\Gamma)$  of a closed  $n$ -chain  $\Gamma = \Gamma_n^{\text{cl}}$  in  $\mathbb{R}^2$ , with length vector  $\vec{\ell}$ , may be parameterized by points  $\vec{\theta}$  in the  $n$ -torus  $\mathbb{T}^n = (S^1)^n$ , where for a configuration  $\mathbf{x} \in \mathcal{C}(\Gamma) \subset \mathcal{C}_*(\Gamma)$ ,  $\vec{\theta}(\mathbf{x}) = (\theta_1, \dots, \theta_n)$  is the vector of angles  $\theta_i$  between  $\mathbf{x}(e_i)$  and the positive  $x$ -axis. This encodes the one-to-one correspondence between a configuration  $\mathbf{x}$  of  $\Gamma$  and the *arrow diagram* obtained by moving all vectors  $\mathbf{x}(e_i)$  to the origin. See Figure 2, where (a) is a configuration of a pentagon, and (b) is the corresponding arrow diagram.

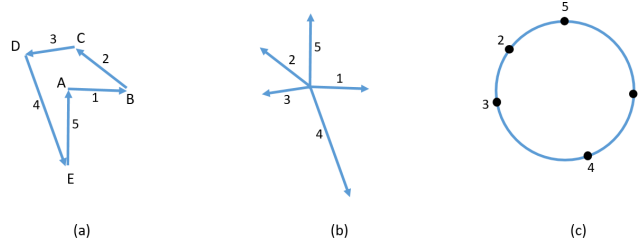


FIGURE 2. Arrow diagram

Of course, not every value of  $\vec{\theta} \in (S^1)^n$  is allowed – we have two constraints,

$$(6) \quad \sum_{i=1}^n \ell_i \cos \theta_i = 0 \quad \text{and} \quad \sum_{i=1}^n \ell_i \sin \theta_i = 0 ,$$

to ensure that the chain is closed.

The reduced configuration space is then  $\widehat{\mathcal{C}}(\Gamma) = \mathcal{C}_*(\Gamma)/\text{SO}(2)$ , with the circle  $\text{SO}(2)$  acting by rotating a configuration about the origin (as in §2.1). It may be parameterized by  $\vec{\theta} \in \mathbb{T}^{n-1}$ , since we fix  $\theta_1 = 0$ . In order for  $\mathbf{x}$  to be fully reduced, we also require that the first  $\theta_i$  ( $i \geq 2$ ) which is not 0 or  $\pi$  must be  $< \pi$ .

#### 4.2. Cells in the torus

The torus  $\mathbb{T}^n$  is decomposed into  $n$ -dimensional cells by (the images of) the hyperplanes in  $\mathbb{R}^n$  given by conditions of the form  $\theta_i = \theta_{i+1}$  or  $\theta_i = \theta_{i+1} + \pi$  for  $1 \leq i \leq n$ . In any connected component  $E$  of the complement of these hyperplanes, we may use any consecutive  $n-3$  of the parameters  $(\theta_1, \dots, \theta_n)$  as local coordinates for  $\widehat{\mathcal{C}}(\Gamma)$  (cf. [F2, Theorem 1.3]). However, we have no control over the intersection of  $E$  with  $\widehat{\mathcal{C}}(\Gamma)$ , which may no longer be connected, for example, so we follow the approach of [KM], in the formulation of [P], to describe a regular cell structure on  $\widehat{\mathcal{C}}(\Gamma)$ .

For this purpose it is convenient to use the homeomorphism  $\phi : S^1 \rightarrow \widehat{\mathbb{R}}$  given by  $\phi(\theta) = \tan(\theta/2)$ , where  $\widehat{\mathbb{R}} := \mathbf{P}\mathbb{R}^1 \cong \mathbb{R} \cup \infty$  is the real projective line. This defines a coordinate-wise identification  $\Phi : \mathbb{T}^n \rightarrow \widehat{\mathbb{R}}^n$  (the  $n$ -fold product), with

$$(7) \quad \vec{t} = (t_1, \dots, t_n) = \Phi(\vec{\theta}) := (\phi(\theta_1), \dots, \phi(\theta_n)).$$

Moreover, since  $\phi(0) = 0$ , the image of  $\widehat{\mathcal{C}}(\Gamma) \subseteq \mathcal{C}_*(\Gamma) \subseteq \mathbb{T}^n$  under  $\Phi$  is contained in  $\{0\} \times \widehat{\mathbb{R}}^{n-1}$ .

Note that the projective special linear group  $\mathrm{PSL}_2(\mathbb{R})$  acts by Möbius transformations on  $\widehat{\mathbb{R}}$ , and thus diagonally on  $\widehat{\mathbb{R}}^n$ . It turns out that the orbit space  $\widehat{\mathbb{R}}^n / \mathrm{PSL}_2(\mathbb{R})$  is isomorphic to  $\widehat{\mathcal{C}}(\Gamma)$  by [KM, Theorem 4] (which is stated in terms of stable measures on  $S^1$ , allowing one to conformally transform any arrow diagram  $\vec{\theta}$  into one with vector sum at the origin).

#### 4.3. Cells for the configuration space of a polygon

As in [P, §1], we first note that for  $\Gamma = \Gamma_n^{\mathrm{cl}}$  an  $n$ -polygon (in  $\mathbb{R}^2$ ), with length vector  $\vec{\ell}$ , we have a dense open subset  $\mathcal{C}_*^o(\Gamma)$  of  $\mathcal{C}_*(\Gamma)$  consisting of those arrow diagrams  $\vec{\theta}$  with all angles distinct. To each such  $\vec{\theta}$  we associate a *cyclic ordering*  $\alpha(\vec{\theta})$  of the arrows, labelled by  $\{1, \dots, n\}$ , on the circle: that is, a coset of the symmetric group  $S_n$  modulo the left action of the subgroup  $C_n$  generated by the cyclic permutation  $(2, 3, \dots, n, 1)$ . This coset is obtained from the given labelling of the arrows by the edges  $(e_1, \dots, e_n)$  of  $\Gamma_n^{\mathrm{cl}}$  by selecting an arbitrary starting point, and the action of  $C_n$  corresponds to choosing a new starting point. See (c) in Figure 2.

Since this process respects the  $\mathrm{SO}(2)$ -action on a pointed configuration  $\mathbf{x} \in \mathcal{C}_*(\Gamma)$ , and thus on  $\vec{\theta}(\mathbf{x})$ , the map  $\alpha : \mathcal{C}_*^o(\Gamma) \rightarrow S_n/C_n$  descends to  $\widehat{\alpha} : \widehat{\mathcal{C}}^o(\Gamma) \rightarrow S_n/C_n$ , where  $\widehat{\mathcal{C}}^o(\Gamma)$  is the corresponding dense open subset of the reduced configuration space  $\widehat{\mathcal{C}}(\Gamma)$ .

The preimage under  $\widehat{\alpha}$  of each coset  $[\sigma] \in S_n/C_n$  is an open cell  $\widehat{E}_\sigma$  in  $\widehat{\mathcal{C}}(\Gamma)$ . Any two such cells are homeomorphic under a relabelling of the arrows, so we may concentrate on the cell  $\widehat{E}_{\mathrm{Id}}$  corresponding to the identity

permutation: thus  $\widehat{E}_{\text{Id}}$  consists of strictly convex configurations of  $\Gamma$  (in the upper half plane).

To see that  $\widehat{E}_{\text{Id}}$  is in fact a regular cell (that is, homeomorphic to a ball, with a regular cell structure on its boundary), we proceed as follows (see [P, Lemma 1.2]):

Note that  $\Phi : \mathbb{T}^n \rightarrow \widehat{\mathbb{R}}^n$  preserves the cyclic order of the coordinates: i.e.,  $\theta_i \prec \theta_j \prec \theta_k$  in the positive direction on  $S^1$  if and only if  $t_i \prec t_j \prec t_k$  in  $\widehat{\mathbb{R}}$ , and this cyclic order on  $\widehat{\mathbb{R}}$  is preserved by Möbius transformations. Moreover, if  $\widehat{E} = \widehat{E}_\sigma$  is any open cell in  $\widehat{\mathcal{C}}(\Gamma) \subseteq \mathbb{T}^n$ , any  $\vec{\theta} \in \widehat{E}$  has pairwise distinct coordinates, so the same is true of the set  $\widehat{E}' := \Phi(\widehat{E})$ . By standard facts about Möbius transformations, for each  $\vec{\mathbf{t}} = \Phi(\vec{\theta}) \in \widehat{E}'$  there is a unique  $\mathcal{P}_{\vec{\mathbf{t}}} \in \text{PSL}_2(\mathbb{R})$  such that  $\mathcal{P}_{\vec{\mathbf{t}}}(t_1) = \infty$ ,  $\mathcal{P}_{\vec{\mathbf{t}}}(t_2) = 0$ , and  $\mathcal{P}_{\vec{\mathbf{t}}}(t_n) = 1$ . It is given by:

$$(8) \quad w = \mathcal{P}(t) := \frac{t - t_2}{t - t_1} \cdot \frac{t_n - t_1}{t_n - t_2},$$

which simplifies when  $t_1 = 0$  to  $\mathcal{P}(t) := \frac{t_n(t-t_2)}{t(t_n-t_2)}$ , with inverse

$$(9) \quad t = \mathcal{P}^{-1}(w) := \frac{t_2 t_n}{(t_2 - t_n)w + t_n}.$$

Moreover, the correspondence  $\mathbf{t} \mapsto \mathcal{P}_{\vec{\mathbf{t}}}$  is continuous and one-to-one.

Thus we have a map  $\mathcal{P} : \widehat{E}' \rightarrow \widehat{\mathbb{R}}^n$ , defined by

$$(10) \quad \mathcal{P}(\vec{\mathbf{t}}) = (\infty, 0, \mathcal{P}_{\vec{\mathbf{t}}}(t_3), \dots, \mathcal{P}_{\vec{\mathbf{t}}}(t_{n-1}), 1)$$

which is a bijection onto its image  $\widehat{E}''$ . Because  $\mathcal{P}_{\vec{\mathbf{t}}}$  preserves the ordering of the coordinates in  $\widehat{\mathbb{R}}$ , we see that for  $\widehat{E} = \widehat{E}_{\text{Id}}$ ,  $\widehat{E}''$  is isomorphic to the affine cell

$$(11) \quad \{ \vec{\mathbf{s}} = (s_3, \dots, s_{n-1}) \in \mathbb{R}^{n-3} \mid 0 < s_3 < s_4 < \dots < s_{n-1} < 1 \}.$$

Since for any cyclic permutation  $\sigma$ ,  $\widehat{E}_\sigma$  is isomorphic to  $\widehat{E}_{\text{Id}}$ , it is also an affine cell under the appropriate identifications.

The top cells in  $\partial \widehat{E}$  correspond to the various cases where two adjacent arrows in  $\vec{\theta}$  coincide, in which case the corresponding configuration  $\mathbf{x} = \mathbf{x}(\vec{\theta})$  is a strictly convex configuration for a closed polygon with  $n-1$  edges, and with length vector  $\vec{\ell}'$  such that  $\ell'_i = \ell_i$  for  $1 \leq i_0$ ,  $\ell'_{i_0} = \ell_{i_0} + \ell_{i_0+1}$  and  $\ell'_i = \ell_{i+1}$  for  $i_0 < i < n$ . Similarly by recursion for the remaining cells in  $\partial \widehat{E}''$ .

In almost all cases these top cells correspond to the analogous boundary cells of  $\widehat{E}''$  with equalities in (11). The cases where  $\theta_1 = \theta_2$ , say, are treated by changing our choice of which coordinates of  $\vec{\mathbf{t}}$  are sent to  $(\infty, 0, 1)$  in (10).

#### 4.4. Cells for the fully reduced configuration space

For the fully reduced case, note that in  $\mathcal{C}_*^o(\Gamma)$  we can also associate to an arrow diagram  $\vec{\theta}$  a coset  $\beta(\vec{\theta})$  of the symmetric group  $S_n$  modulo the left action of the dihedral subgroup  $D_n$ , which acts on a labelling of the arrows in  $\vec{\theta}$  by varying both the starting point and the direction in which we proceed. Since  $C_n < D_n$ , we have a surjection  $\pi : S_n/D_n \rightarrow S_n/C_n$ , with  $\alpha = \pi \circ \beta$ . We call  $\beta(\vec{\theta})$  the *dihedral ordering* associated to  $\vec{\theta}$ .

Again, this process respects the  $O(2)$ -action on a pointed configuration  $\mathbf{x} \in \mathcal{C}_*(\Gamma)$ , and thus on  $\vec{\theta}(\mathbf{x})$ , so  $\beta : \mathcal{C}_*^o(\Gamma) \rightarrow S_n/D_n$  induces  $\hat{\beta} : \hat{\mathcal{C}}^o(\Gamma) \rightarrow S_n/C_n$ , where  $\tilde{\mathcal{C}}^o(\Gamma)$  is the corresponding dense open subset of the fully reduced configuration space  $\tilde{\mathcal{C}}(\Gamma)$ .

Note that we have a trivial double covering map  $\delta^o : \hat{\mathcal{C}}^o(\Gamma) \rightarrow \tilde{\mathcal{C}}^o(\Gamma)$ , although the corresponding map  $\delta : \hat{\mathcal{C}}(\Gamma) \rightarrow \tilde{\mathcal{C}}(\Gamma)$  has branch points at fully aligned configurations of  $\Gamma$  (if they exist, as for even equilateral polygons).

Thus the preimage under  $\hat{\beta}$  of each coset  $[\sigma] \in S_n/D_n$  is again an open cell  $\tilde{E}_\sigma$  in  $\tilde{\mathcal{C}}(\Gamma)$ , doubly covered by  $\hat{E}_{\sigma'} \amalg \hat{E}_{\sigma''}$ , where  $\{[\sigma'], [\sigma'']\} = \pi^{-1}[\sigma]$ . We must be more careful in analyzing the boundary  $\partial\tilde{E}_\sigma$ , since  $\delta : \hat{\mathcal{C}}(\Gamma) \rightarrow \tilde{\mathcal{C}}(\Gamma)$  may have branch points there.

### 5. Automorphisms of planar polygons

In Section 4 we summarized briefly the standard approach to describing the cell structure of the (fully) reduced configuration spaces of polygons in the plane. We now turn to a finer cell structure needed to analyze the symmetric configuration spaces. First, we note a straightforward result about  $\text{Aut}(\Gamma)$ , for closed chains  $\Gamma$ :

**Definition.** Let  $\hat{\ell}$  be the cyclic word in  $n$  positive real numbers corresponding to the (ordered) length vector  $\vec{\ell}$ . The maximal number  $k \geq 1$  of repeating segments  $I$  into which  $\hat{\ell}$  can be divided will be called the *order* of  $\vec{\ell}$  (so  $k|n$ ).

If  $\hat{\ell}$  is symmetric (with respect to reversing the order from a certain starting point), we call  $\vec{\ell}$  *palindromic*. More generally, if after possibly omitting a single length  $\ell_i$  from  $\hat{\ell}$  it becomes palindromic, we say that  $\vec{\ell}$  is *reflective*. Thus  $\hat{\ell} = (1, 2, 3, 2, 1)$  is palindromic, while  $(1, 2, 3, 2, 1, 4)$  is reflective.

**Lemma 5.1.** *Given a length vector  $\vec{\ell}$  a closed chain  $\Gamma = \Gamma_n^{\text{cl}}$  of length  $n$ , the automorphism group of the linkage  $\Gamma$  is*

$$\text{Aut}(\Gamma) \cong \begin{cases} D_k & \text{if } \vec{\ell} \text{ is reflective} \\ C_k & \text{if } \vec{\ell} \text{ is not reflective,} \end{cases}$$

where  $D_n$ , the dihedral group of order  $2n$ , is the group of symmetries of the equilateral  $n$ -gon  $\Gamma_n^{\text{eq}}$ , so in particular  $D_2 := C_2$  and  $C_1 = \{1\}$ .

*Proof.* If  $k \geq 2$  and  $\vec{\ell}$  is non-reflective, rotation along the repeated segment  $I$  generates  $\text{Aut}(\Gamma) = C_k$ .

If  $\vec{\ell}$  is reflective, we have in addition a reflection in an axis which either connects two opposite vertices  $u$  and  $v$  (if  $n$  is even and  $\vec{\ell}$  is palindromic starting at  $u$ ); connects a vertex to the midpoint of an edge (if  $n$  is odd and  $\vec{\ell}$  is palindromic); or connects the midpoints of two opposite edges  $e$  and  $f$  (if  $n$  is even and  $\vec{\ell}$  is palindromic after dropping  $e$ , say). If also  $k \geq 2$ , we have a total of  $k$  possible reflections of this form.  $\square$

### 5.1. $\text{Aut}(\Gamma)$ -cells

The key to understanding the symmetric configuration space is using appropriate cells for the description of the reduced configuration space  $\widehat{\mathcal{C}}(\Gamma)$ , and its fully reduced version  $\widetilde{\mathcal{C}}(\Gamma)$ , which take into account the  $\text{Aut}(\Gamma)$ -action. More precisely, we decompose  $\widehat{\mathcal{C}}(\Gamma)$  (or  $\widetilde{\mathcal{C}}(\Gamma)$ ) into open *free*  $H$ -cells for each subgroup  $H$  of  $\text{Aut}(\Gamma)$  – that is, open cells of the form  $\mathbf{e}^n \times H$ , with the  $H$  acting on the second coordinate (see [Ma]).

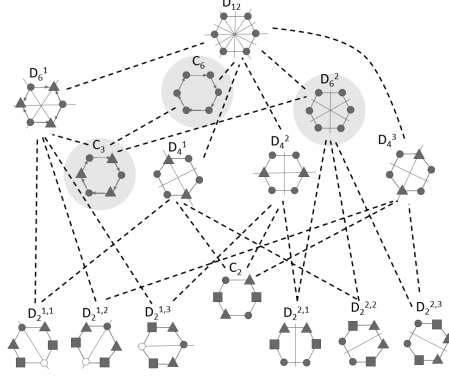
The highest dimensional cells in this decomposition (with  $\dim(C_{\mathcal{X}}) = n-3$ ) will be those for which the action of  $\text{Aut}(\Gamma)$  is free (in the interior). This simply reflects the fact that generic configurations have no symmetries, if  $n \geq 5$  (which fails for the equilateral quadrilateral, as we see in Lemma A.7). Note, however, that the action may take an open cell  $\widehat{E}_\sigma$  to itself; to avoid this, we must subdivide it into finer (open) cells which are permuted among themselves by  $\text{Aut}(\Gamma)$  (acting under relabelling combined with normalization back to the reduced form).

These fine cells are determined by “breaking the symmetry” of the corresponding arrow diagram – that is, imposing an additional (open) condition which determines a unique “canonical” labelling of the vertices.

*Remark 5.2.* The subgroup lattice of  $\text{Aut}(\Gamma)$  plays a central role in our analysis of the equivariant cell structure. Note, however, that for certain subgroups  $H$  of  $\text{Aut}(\Gamma)$ , any configuration stabilized by  $H$  are in fact invariant under a larger subgroup. Thus for example when  $\Gamma = \Gamma_6^{\text{eq}}$  is the equilateral hexagon, the three subgroups shaded in the lattice of subgroups of  $\text{Aut}(\Gamma) = D_{12}$  in Figure 3 will never appear as stabilizers.

**Definition.** Consider an open cell  $\widehat{E}_\sigma$  for  $\widetilde{\mathcal{C}}(\Gamma)$  corresponding to a cyclic (or dihedral) ordering  $[\sigma]$  in  $S_n/C_n$  (or  $S_n/D_n$ ) – see §4.4.

It is convenient to think of our geometric representation of the abstract cyclic (or dihedral) ordering  $[\sigma] \in S_n/D_n$  as a certain (fully) reduced configuration of a mechanism  $\Delta_n$  consisting of  $n$  unit vectors emanating from the same point in the plane. Since we are only interested in the cyclic ordering, we choose a normalized representative  $c_\sigma$  in  $\widehat{\mathcal{C}}(\Delta_n)$  (respectively,  $\widetilde{\mathcal{C}}(\Delta_n)$ ) for  $[\sigma]$  in which the arrow heads lie at the cyclotomic points  $c_k = \frac{2(k-1)\pi}{n}$  ( $k = 1, \dots, n$ ), suitably labelled, with  $\sigma(1) = 1$ .

FIGURE 3. Subgroup lattice of  $D_{12}$ 

The action of  $\psi \in \text{Aut}(\Gamma) \subseteq D_n$  is by changing the labelling  $\sigma(k)$  of  $c_k$  to  $\psi(\sigma(k))$ , and then renormalizing by applying a cyclic shift to  $\psi \circ \sigma$  to obtain a new permutation  $\sigma'$  with  $\sigma'(1) = 1$  (the label of  $c_1$ ), for a cyclic ordering.

In the case of a dihedral ordering, we further normalize by requiring that  $\sigma'(2)$  appear as the label of a cyclotomic point in the upper half-plane (unless it is at  $c_{n/2} = \pi$ , in which case  $\sigma'(3)$  must be in the upper half-plane).

We denote the subgroup of  $\text{Aut}(\Gamma)$  fixing a given cyclic (or dihedral) ordering  $[\sigma]$  by  $\text{Aut}([\sigma])$ . Thus  $\psi \in \text{Aut}([\sigma])$  if and only if  $\sigma' = \sigma$ .

## 5.2. Fine cells

Note that  $\text{Aut}(\Gamma)$  acts freely on the dense open subspace  $\tilde{\mathcal{C}}^\circ(\Gamma)$ , but  $\text{Aut}([\sigma])$  takes the open cell  $\tilde{E}_\sigma$  to itself. Thus the cardinality  $N$  of  $\text{Aut}([\sigma])$  is the number of fine cells into which we must divide  $\tilde{E}_\sigma$ .

To specify such a fine cell, we think of  $\text{Aut}([\sigma])$  as a subgroup of the cyclic group  $C_n$  (or the dihedral group  $D_n$ , in the fully reduced case), now acting in the standard way on the regular  $n$ -gon (or the cyclotomic points on the circle). Each orbit under this action imposes a (different) partition of  $\tilde{E}_\sigma$  into fine cells, defined as follows:

- (a) If  $\text{Aut}([\sigma])$  is cyclic of order  $N$ , generated by

$$\psi \in \text{Aut}([\sigma]) \subseteq \text{Aut}(\Gamma) \subseteq D_{2n} \subseteq \text{Aut}(\Delta_n) = S_n$$

(which is always true for the reduced configuration space), then  $\psi$  acts on (the labelling of) the cyclotomic points  $(c_k)_{k=1}^n$  as a rotation by an angle of  $\frac{2\pi}{N}$ , so the orbit of  $c_\ell$  under this action is  $\alpha = (c_{i_k})_{k=1}^N$ , where  $i_k = \ell + (k-1)N \pmod{n}$ .

For each such orbit  $\alpha$ , we define one (open) fine cell  $\hat{F}_\sigma(i_k, i_{k+1})$  of  $\hat{E}_\sigma$  for each element  $c_{i_k}$  in the orbit: this consists of those



configurations (angle sets)  $\vec{\theta} \in \widehat{E}_\sigma$  for which the angle  $|\theta_{i_k} - \theta_{i_{k+1}}|$  is strictly smaller than  $|\theta_{i_j} - \theta_{i_{j+1}}|$  for all  $1 \leq j \neq k \leq N$ .

The same rule applies for the subdivision of  $\widetilde{E}_\sigma$  in  $\widetilde{\mathcal{C}}^o(\Gamma)$  into fine cells  $\widetilde{F}_\sigma(i_k, i_{k+1})$ .

- (b) If  $\text{Aut}([\sigma])$  is dihedral of order  $N = 2M$  (necessarily in the fully reduced case), we distinguish three cases:
- (i) If we have an orbit with three neighboring cyclotomic points, it necessarily includes *all* the cyclotomic points – in other words,  $\sigma$  is the identity permutation, and the open cell  $\widetilde{E}_\sigma$  is divided into  $N$  fine cells. These may be distinguished by specifying for which  $1 \leq k \leq N$  the angle  $\theta_k - \theta_{k+1}$  is smallest, and then further dividing this set into two subcells by the two possible orderings of  $|\theta_{k+1} - \theta_{k+2}|$  and  $|\theta_{k-1} - \theta_k|$ . This will determine a canonical labelling of each configuration  $\mathbf{x} \in \widetilde{E}_\sigma$  in the fine cell  $\widetilde{F}_\sigma(i_k, i_{k-1})$ , starting at the  $i_k$ -th vertex in the direction  $i_k \mapsto i_{k-1}$ ; similarly  $\widetilde{F}_\sigma(i_k, i_{k+1})$  for the other.
  - (ii) If we have an orbit with exactly two neighboring cyclotomic points – so the whole orbit consists of such pairs  $(i_k, i_{k+1})$  ( $k = 1, \dots, M$ ) – we may again name a fine cell  $\widetilde{F}_\sigma(i_k, i_k - 1)$ , say, by specifying which  $i_k$  has the smallest angle difference between  $\theta_{i_k}$  and its cyclotomic neighbor  $\theta_{i_k \pm 1}$  which is *not* in the orbit.
  - (iii) If we have an orbit with no neighboring cyclotomic points, we may name a fine cell  $\widetilde{F}_\sigma(i_k, i_k - 1)$  or  $\widetilde{F}_\sigma(i_k, i_k + 1)$  by specifying which  $i_k$  has the smallest angle  $|\theta_{i_k} - \theta_{i_k \pm 1}|$ , as in (i).

**Definition.** For each open cell  $\widehat{E}_\sigma$  of  $\widehat{\mathcal{C}}(\Gamma)$  corresponding to a cyclic ordering  $[\sigma]$  as above, the *membrane* separating two fine cells  $\widehat{F}_\sigma(i_k, i_{k+1})$  and  $\widehat{F}_\sigma(j_m, j_{m+1})$  is the subset  $\mathcal{M} = \widehat{F}_\sigma(i_k, i_{k+1}) \cap \widehat{F}_\sigma(j_m, j_{m+1})$  determined by the condition

$$(12) \quad |\theta_{i_k} - \theta_{i_{k+1}}| = |\theta_{j_m} - \theta_{j_{m+1}}|.$$

Similarly, for each open cell  $\widetilde{E}_\sigma$  of  $\widetilde{\mathcal{C}}(\Gamma)$  corresponding to a dihedral ordering  $[\sigma]$ , the *membrane* separating two fine cells  $\widetilde{F}_\sigma(i_k, i_{k'})$  and  $\widetilde{F}_\sigma(j_m, j_{m'})$  is the subset  $\mathcal{M} = \widetilde{F}_\sigma(i_k, i_{k'}) \cap \widetilde{F}_\sigma(j_m, j_{m'})$  determined by one of two conditions:

- (a) If  $i_k = j_m$ , necessarily  $k' \neq m'$  – say,  $k' = k - 1$  and  $m' = m + 2$  – and  $\mathcal{M}$  is then determined by the condition

$$(13) \quad |\theta_{i_k} - \theta_{i_{k-1}}| = |\theta_{j_{m+1}} - \theta_{j_{m+2}}|.$$

- (b) If  $i_k \neq j_m$ ,  $\mathcal{M}$  is determined by the condition

$$(14) \quad |\theta_{i_k} - \theta_{i_{k+1}}| = |\theta_{j_m} - \theta_{j_{m+1}}|.$$

**Theorem 5.3.** *If  $\Gamma = \Gamma_n^{\text{cl}}$  is a closed  $n$ -chain with length vector  $\vec{\ell}$ , its reduced configuration space  $\widehat{\mathcal{C}}(\Gamma)$  has a regular  $\text{Aut}(\Gamma)$ -equivariant cell structure, subordinate to the fine cell decomposition of §5.2, and thus to the regular cell structure of  $[P]$ .*

*Proof.* Since the membranes are (codimension 1) subspaces of the open cells  $\widehat{E} = \widehat{E}_\sigma$  in the dense open set  $\widehat{\mathcal{C}}^\circ(\Gamma) \subseteq \widehat{\mathcal{C}}(\Gamma)$ , we may use the identifications  $\widehat{E} \xrightarrow{\Phi} \widehat{E}' \xrightarrow{\mathcal{P}} \widehat{E}''$  to try to describe the membrane  $\mathcal{M}$  using the chosen affine coordinates for  $\widehat{E}''$ .

Since  $\vec{t} = (t_1, \dots, t_n) = \Phi(\vec{\theta})$  for  $t_i = \tan \frac{\theta_i}{2}$ , using the formula

$$\tan(\alpha - \beta) = \frac{\tan(\alpha) - \tan(\beta)}{1 + \tan(\alpha) \cdot \tan(\beta)},$$

we see that (12) takes the form:

$$(15) \quad \frac{t_{i_k} - t_{i_{k+1}}}{1 + t_{i_k} \cdot t_{i_{k+1}}} = \frac{t_{j_m} - t_{j_{m+1}}}{1 + t_{j_m} \cdot t_{j_{m+1}}}$$

(assuming for the moment that  $\theta_{i_k} > \theta_{i_{k+1}}$  and  $\theta_{j_m} > \theta_{j_{m+1}}$ ).

For simplicity, let  $i_k = i_1 = 1$  (so  $t_1 = 0$ ): writing  $i = i_k + 1$ ,  $j = j_m$ , and  $k = j_m + 1$ , (15) simplifies to:

$$(16) \quad t_i \cdot t_j \cdot t_k = t_k - t_j - t_i.$$

If we further assume that  $\{i, j, k\} \cap \{1, 2, n\} = \emptyset$  (after identifying  $\widetilde{E}_\sigma$  with  $\widetilde{E}_{\text{Id}}$  under an appropriate relabelling of the arrows), then  $\theta_i$ ,  $\theta_j$ , and  $\theta_k$  are taken under  $\mathcal{P}$  to the corresponding coordinates  $(s_i, s_j, s_k)$  in the affine cell  $\widetilde{E}''$ , as in (11).

Substituting the values for (9) into (16) yields:

$$(17) \quad \frac{t_2^3 t_n^3}{((t_2 - t_n)s_i + t_n) \cdot ((t_2 - t_n)s_j + t_n) \cdot ((t_2 - t_n)s_k + t_n)} \\ = \frac{t_2 t_n}{(t_2 - t_n)s_k + t_n} - \frac{t_2 t_n}{(t_2 - t_n)s_j + t_n} - \frac{t_2 t_n}{(t_2 - t_n)s_i + t_n},$$

or, after cross-multiplying:

$$(18) \quad t_2^2 t_n^2 = ((t_2 - t_n)s_i + t_n) \cdot ((t_2 - t_n)s_j + t_n) \\ - ((t_2 - t_n)s_i + t_n) \cdot ((t_2 - t_n)s_k + t_n) \\ - ((t_2 - t_n)s_j + t_n) \cdot ((t_2 - t_n)s_k + t_n)$$

Note that if  $t = \tan(\theta/2)$  then (by the usual rational parametrization of  $S^1$ ):

$$(19) \quad \cos \theta = \frac{1 - t^2}{1 + t^2} \quad \text{and} \quad \sin \theta = \frac{2t}{1 + t^2},$$

so (6) becomes:

$$(20) \quad \sum_{i=1}^n \ell_i \cdot \frac{1-t_i^2}{1+t_i^2} = 0 \quad \text{and} \quad \sum_{i=1}^n \ell_i \cdot \frac{2t_i}{1+t_i^2} = 0.$$

Setting  $t_1 = 0$ , and substituting:

$$(21) \quad t_i = \frac{t_2 t_n}{(t_2 - t_n) s_i + t_n}.$$

from (9) into (20) for  $i = 3, \dots, n-1$ , we obtain two equations involving  $\{t_1 = 0, t_2, s_3, \dots, s_{n-1}, t_n\}$ . We can solve these for  $t_2$  and  $t_n$ , obtaining an algebraic equation for the membrane in the variables  $\vec{s} = (s_3, \dots, s_{n-1})$  from (17). The fine cells bounded by this membrane are therefore semi-algebraic sets inside the affine sets (thought of as open subsets of the standard affine space  $\mathbb{R}^{n-3}$ ), in which the equalities (12), (13), and (14), are replaced by inequalities.

We may now use Hironaka's result on triangulating real semi-algebraic sets (see [Hi]) to obtain the required triangulation, which can be made compatible with that of the boundaries by [L]. We do so by induction on the dimension of the naive cells: the main point to keep in mind is that once we choose a triangulation for one of the fine cells, on one side of a membrane, we may reproduce it for all the others using the free action of  $\text{Aut}(\Gamma)$  on the interior (and the fact that this action is compatible with that on the boundary of the fine cell, which may not be free).  $\square$

**Corollary 5.4.** *For  $\Gamma = \Gamma_n^{\text{cl}}$  as above, the fully reduced configuration space  $\tilde{\mathcal{C}}(\Gamma)$  also has a regular  $\text{Aut}(\Gamma)$ -equivariant cell structure, compatible with that of  $\hat{\mathcal{C}}(\Gamma)$  in Theorem 5.3.*

*Proof.* The  $C_2$ -action on  $\hat{\mathcal{C}}(\Gamma)$  by reflections in the  $x$ -axis generally switches two distinct cells in the regular cell structure of Section 4, thus form a double cover of a single cell in  $\tilde{\mathcal{C}}(\Gamma)$ . The only cells fixed by the  $C_2$ -action are vertices corresponding to linear configurations (with all adjacent angles 0 or  $\pi$ ), and these can be dealt with as in [P, §4] (see also [GP]).  $\square$

## 6. Symmetric configurations for planar polygons

In Section 5 we described a process for producing an equivariant cell structure for the (fully) reduced configuration space of a planar polygon, based on a refinement of the non-equivariant regular cell structure described in Section 4. When the  $\text{Aut}(\Gamma)$ -action on the fine cells is free, the orbit yields a single cell in the associated symmetric configuration space  $\tilde{\mathcal{S}}\mathcal{C}(\Gamma)$ . As noted above, this will happen in the interior of the top dimensional cells. However, in the lower dimensional cells, occurring in the boundary of those with free action, we may have fixed points. From the proof of Theorem 5.3 we see that in fact we must start from the lowest dimensional cells in constructing our equivariant cell

structure. Thus, we need to understand the *symmetric* configurations: those fixed under a subgroup  $H$  of  $\text{Aut}(\Gamma)$ . In particular, these will be needed in order to obtain a compatible decomposition of  $\widetilde{\mathcal{SC}}(\Gamma)$ .

By Lemma 5.1, for any  $n$ -polygon  $\Gamma$  the automorphism group  $\text{Aut}(\Gamma)$  is either cyclic or dihedral, so the same is true for any subgroup  $H \leq \text{Aut}(\Gamma)$ . We must consider three cases:

**Case I.** Cyclic subgroup of  $\text{Aut}(\Gamma)$  generated by a reflection:

Assume first that the subgroup  $H$  is generated by a reflection  $\rho \in \text{Aut}(\Gamma)$ , in an axis of symmetry  $\lambda$  for the labels  $(A_1, \dots, A_n)$  of  $\Gamma$ . As noted in the proof of Lemma 5.1, this can have three forms:

- (1) If  $n = 2k + 1$  is odd,  $\rho$  is a reflection in a *median* connecting  $A_{k+1}$  with the midpoint of  $A_n A_1$ , say, so  $\rho(A_i) = A_{n+1-i}$  ( $i = 1, \dots, k + 1$ ).
- (2) If  $n = 2k$  is even,  $\rho$  may be a reflection in
  - (i) a *diagonal*, connecting  $A_1$  with  $A_{k+1}$ , say, so  $\rho(A_i) = A_{n+2-i}$  (indices taken modulo  $n$ ).
  - (ii) a *midsegment*, connecting the midpoint of  $A_n A_1$  with that of  $A_k A_{k+1}$ , say, so  $\rho(A_i) = A_{n+1-i}$ .

**Proposition 6.1.** *Let  $\Gamma = \Gamma_n^{\text{cl}}$  be a planar  $n$ -polygon, with  $H = C_2 \leq \text{Aut}(\Gamma)$  generated by a reflection in the axis  $\lambda$ . We then have a map  $\phi : \widetilde{\mathcal{C}}(\Gamma)^H \rightarrow \widetilde{\mathcal{C}}(\Gamma_k^{\text{op}})$  from the fixed-point set, where:*

- (1) *If  $n = 2k + 1$  and  $\lambda$  is a median to  $AB$ ,  $\Gamma_k^{\text{op}}$  is either half of  $\Gamma' = \Gamma \setminus (AB)$ , and  $\phi$  is one-to-one.*
- (2) *If  $n = 2k$  and  $\lambda$  is a diagonal,  $\Gamma_k^{\text{op}}$  is either half of  $\Gamma$ , and  $\phi$  is one-to-one except over  $\Gamma_k^{\text{cl}}$  (the subspace of chains which close up), where the fiber is  $\mathbf{PR}^1$ .*
- (3) *If  $n = 2k + 2$  is even and  $\lambda$  is a midsegment from  $AB$  to  $CD$ ,  $\Gamma_k^{\text{op}}$  is either half of  $\Gamma' = \Gamma \setminus (AB), (CD)$ , and  $\phi$  is a double cover.*

*Proof.* In each case, by reflecting a given configuration for the open chain  $\Gamma_k^{\text{op}}$  about the geometric axis of symmetry  $L$ , we obtain a unique symmetric configuration for  $\Gamma$ .

- (1) When  $\lambda$  is a median,  $L$  is the  $y$ -axis (the perpendicular bisector of  $AB$ ) in the fully reduced case. We may then rotate any configuration for  $\Gamma_k^{\text{op}}$  about  $B$  until it touches  $L$ .
- (2) When  $\lambda$  is a diagonal  $AD$ , say, for any configuration  $\mathbf{x}$  of the open chain  $\Gamma_k^{\text{op}}$  we let  $L$  be the line from  $\mathbf{x}(A)$  to  $\mathbf{x}(D)$ ; however, when these two coincide we may choose  $L$  at will from  $\mathbf{PR}^1$ .
- (3) When  $\lambda$  is a midsegment from  $AB$  to  $CD$ ,  $L$  is the perpendicular bisector of  $AB$ ; let  $L'$  and  $L''$  be the two parallels to  $L$  at distance  $\frac{1}{2}d(C, D)$ , and then rotate any configuration for  $\Gamma_k^{\text{op}}$  about  $B$  until it touches  $L'$  or  $L''$ .

See Figure 4 for the third case.  $\square$

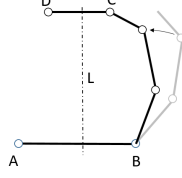


FIGURE 4. Midsegment reflection

*Remark 6.2.* In principle, we would like to relate the analysis of the symmetric configurations in  $\widehat{\mathcal{C}}(\Gamma)$  or  $\widetilde{\mathcal{C}}(\Gamma)$  with the fine cell structure introduced in Section 5. This would require a better understanding of the triangulation described in Theorem 5.3. However, it is possible to use Proposition 6.1 to study the action of  $\text{Aut}(\Gamma)$  on the open cell  $E = E_{\text{Id}}$  of (strictly) convex configurations, under a single reflection  $\rho \in \text{Aut}(\Gamma)$  in an axis of symmetry  $\lambda$  for the labels  $(A_1, \dots, A_n)$  of  $\Gamma$ .

The set  $D$  of convex configurations  $\mathbf{x} \in E$  which are fixed under  $\rho$  must also be symmetric in the geometric sense, with axis of symmetry  $L$  realizing  $\lambda$ . Such a configuration is completely described by the half on one side of  $L$ , which is simply a fully reduced convex configuration  $\mathbf{y}$  for an open chain of length  $k \approx \frac{n}{2}$ . As in §2.1, we parameterize such a  $\mathbf{y}$  by  $\vec{\theta}(\mathbf{y}) = (\theta_1, \dots, \theta_k)$ , (see §4.1), with

$$0 = \theta_1 < \theta_2 < \dots < \theta_k < \pi .$$

Switching to the parametrization (7), we have:

**Lemma 6.3.** *The set of strictly convex fully reduced configurations of a closed chain  $\Gamma = \Gamma_n^{\text{cl}}$  symmetric with respect to a reflection in  $L$  as above are parameterized by*

$$(22) \quad \vec{\mathbf{t}} = (t_1, \dots, t_k) = (\tan(\theta_1/2), \dots, \tan(\theta_k/2)) .$$

with  $0 = t_1 < t_2 < \dots < t_k < \infty$ .

The precise value of  $k$  will appear in the proof.

*Proof.* As in (20), we may calculate the vector sum of the arrow diagram  $\vec{\theta}$ , using the length vector  $\vec{\ell}$  for  $\Gamma$ , by

$$(23) \quad \vec{\mathbf{v}} := \left( \sum_{i=1}^k \ell_i \cdot \frac{1-t_i^2}{1+t_i^2}, \sum_{i=1}^k \ell_i \cdot \frac{2t_i}{1+t_i^2} \right) = (a, b) = \mu(\cos \theta, \sin \theta) ,$$

where  $\mu = \sqrt{a^2 + b^2}$  and  $\theta = \arctan(b/a)$ .

We distinguish three cases in calculating the slope  $\tau$  of  $L$  from  $\vec{\mathbf{t}}$ :

- (1) If  $n = 2k + 1$  and  $L$  is the perpendicular from  $\mathbf{y}(A_k) = \vec{\mathbf{v}}$  to the midpoint of  $\mathbf{y}(e_n)$  (because of the symmetry of  $\mathbf{y}$ ), which has length  $\ell_n$  and forms an (unknown) angle of  $\theta_n$  with the positive  $x$  axis, so  $L$  forms an angle of  $\theta_n - \pi/2$ . Since  $L$ ,  $\vec{\mathbf{v}}$ , and  $\mathbf{y}(e_n)$  form a right triangle with hypotenuse  $\mu$  and edge  $\ell_n/2$  facing the angle  $\alpha = \pi/2 + \theta - \theta_n$ , with  $\sin \alpha = \frac{\ell_n/2}{\mu}$ . This allows us to recover  $\alpha$ , and thus  $\theta_n$  and find the slope of  $L$ , from which we can recover the remaining angles  $\theta_{k+1}, \dots, \theta_{n-1}$ .
- (2) If  $n = 2k$  and  $L$  is a diagonal, its direction is the vector  $\vec{\mathbf{v}}$  of (23), from which we can calculate  $\theta_{k+1}, \dots, \theta_n$  by reflecting  $\theta_1, \dots, \theta_k$  in  $L$ .
- (3) If  $n = 2(k + 1)$  and  $L$  is the perpendicular bisector of  $\mathbf{y}(e_{k+1})$  and  $\mathbf{y}(e_n)$ , it forms an angle  $\alpha$  with  $\vec{\mathbf{v}}$ , with  $\sin \alpha = \frac{|\ell_n/2 - \ell_{k+1}/2|}{\mu}$ , from which we can calculate  $\alpha$ , and thus the remaining angles  $\theta_{k+1}, \dots, \theta_n$ .  $\square$

**Case II.** Cyclic subgroup of  $\text{Aut}(\Gamma)$  generated by a rotation:

In the case where the cyclic subgroup  $H \leq \text{Aut}(\Gamma)$  is generated by a rotation we have:

**Proposition 6.4.** *Let  $\Gamma$  be a planar  $n$ -polygon and  $H = C_d$  a rotation subgroup of  $\text{Aut}(\Gamma)$ , which we identify with a subgroup of  $D_{2d}$  for  $d|n$ , and let  $k := n/d$ . The fixed-point set  $\tilde{\mathcal{C}}(\Gamma)^H$  is isomorphic to a disjoint union, indexed by the discrete set  $\tilde{\mathcal{C}}(\Gamma_d^{\text{eq}})^H$ , of copies of  $\hat{\mathcal{C}}(\Gamma_k^{\text{op}})$ , unless  $\tilde{\mathbf{z}} \in \tilde{\mathcal{C}}(\Gamma_d^{\text{eq}})^H$  is collinear, in which case we replace  $\hat{\mathcal{C}}(\Gamma_k^{\text{op}})$  by  $\tilde{\mathcal{C}}(\Gamma_k^{\text{op}})$ .*

*Proof.* Note that  $H$  is of index 2 in  $D_{2d}$ , which we identify with the automorphism group of the equilateral polygon  $\Gamma_d^{\text{eq}}$  with  $d$  edges of length  $L$  (unless  $d = 2$ , in which case  $H = D_{2d}$ ).

Any fully reduced configuration  $\tilde{\mathbf{x}} \in \tilde{\mathcal{C}}(\Gamma)$  is determined by its restriction to an open subchain  $\Delta$  of  $\Gamma$  with  $k = n/d$  edges, yielding a reduced configuration  $\hat{\mathbf{y}}$  for  $\Delta$ , together with a fully reduced configuration  $\tilde{\mathbf{z}}$  for  $\Gamma_d^{\text{eq}}$ , with  $L$  equal to the distance between the start and end points of  $\hat{\mathbf{y}}$ . Here  $\tilde{\mathbf{z}}$  must be fixed under all (geometric) rotations of  $\Gamma_d^{\text{eq}}$ , and thus under the full automorphism group  $\text{Aut}(\Gamma_d^{\text{eq}}) = D_{2d}$ , since the angles at all vertices of the polygon must be equal.

The fact that  $\hat{\mathbf{y}}$  need not be *fully* reduced means that we will generally have two fully reduced configurations  $\pm \hat{\mathbf{y}}$  attached to each fully symmetric configuration of  $\Gamma_d^{\text{eq}}$ .

Thus for the icosagon  $\Gamma_{20}^{\text{eq}}$ , we have four configurations fixed under  $C_5$  for a given (non-collinear) fully reduced open chain configuration  $\tilde{\mathbf{y}}$  of length 4, ‘attached’ to the regular pentagon and pentagram on either side, as shown in Figure 5, where each of the two pairs (a)-(b) and (c)-(d) correspond to the reduced configurations  $\pm \tilde{\mathbf{y}}$ .

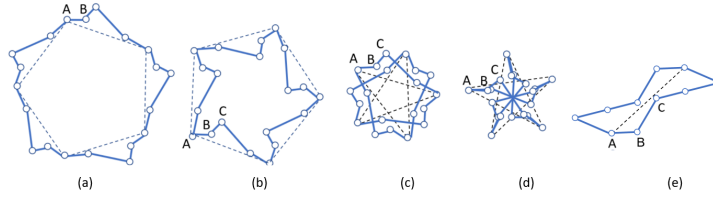


FIGURE 5. Symmetric configurations for the icosagon and decagon

On the other hand, the (fully reduced)  $C_2$ -configuration for the decagon shown in Figure 5(e) is the same for  $\pm\tilde{\mathbf{y}}$ , so it requires only the fully reduced open loop  $\tilde{\mathbf{y}}$ .

Note that even when  $L = 0$  (that is,  $\hat{\mathbf{y}}$  is actually a closed loop), we still have distinct configurations  $\hat{\mathbf{z}}$  corresponding to different reduced symmetric configurations  $\hat{\mathbf{z}}$ : e.g., when  $d = 5$ , the convex pentagon and the pentagram of Figure 12 correspond to two different cyclic arrangements of the petals of the bouquet of five such loops. It might be useful to think of the common endpoints of all the closed loops as an infinitesimal reduced symmetric configuration, in order to keep track of the orientations of the various loops. This is illustrated by the five closed-loop configurations shown in Figure 6, corresponding respectively to those of Figure 5, with the inner dashed symmetric configuration reduced to a point.

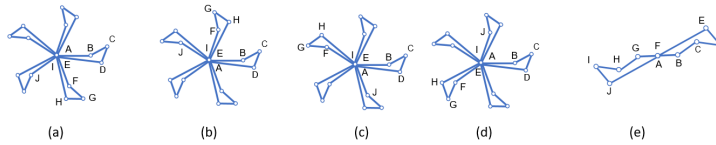


FIGURE 6. Closed loop configurations for the icosagon and decagon

□

**Example 6.5.** When  $d = 6$ , the three possible configurations of the equilateral hexagon  $\Gamma_6^{\text{eq}}$  which are invariant under the full automorphism group  $D_{12} = \text{Aut}(\Gamma_6^{\text{eq}})$  are the first three in the top row of Figure 10 (see Remark 7.1).

**Corollary 6.6.** For  $\Gamma$ ,  $H = C_d$  and  $k = n/d$  as above, the interior of  $\tilde{\mathcal{C}}(\Gamma)^H$  has the same local parametrization as  $\tilde{\mathcal{C}}(\Gamma_k^{\text{op}})$  (see §2.1).

The case where the cyclic subgroup  $H \leq \text{Aut}(\Gamma)$  is generated by a rotation is in fact the only one relevant to the reduced configuration space  $\tilde{\mathcal{C}}(\Gamma)$ , where we have the following somewhat simpler result:

**Proposition 6.7.** *If  $\Gamma$  is a planar  $n$ -polygon and  $H = C_d$  is a rotation subgroup of  $\text{Aut}(\Gamma)$ , the fixed-point set  $\tilde{\mathcal{C}}(\Gamma)^H$  is isomorphic to a disjoint union, indexed by the discrete set  $\tilde{\mathcal{C}}(\Gamma_d^{\text{eq}})^H$ , of copies of  $\tilde{\mathcal{C}}(\Gamma_k^{\text{op}})$ .*

**Case III.** Dihedral subgroups:

Let  $\Gamma$  be a planar  $n$ -polygon,  $H \cong D_{2d}$  a dihedral subgroup of  $\text{Aut}(\Gamma) \subseteq D_{2n}$ , with  $d|n$ . Choose two generators  $\rho$  and  $\sigma$  for  $H$ , which we may identify with reflections in axes  $k$  and  $m$ , respectively, in a regular  $n$ -gon  $\Gamma_n$ . Here we identify  $H$  with a subgroup of  $D_{2n}$ , even though  $\Gamma$  need not be equilateral, in order to have a consistent description of its automorphisms (acting on a fully reduced configuration by relabelling).

If  $n$  is odd, each axis is necessarily a median (connecting a vertex of  $\Gamma$  to the midpoint of the opposite edge). If  $n$  is even, the axis could be a midpoint interval (connecting the midpoints of two opposite edges) or a diagonal connecting two opposite vertices.

The generator  $\rho$  has a “basic subchain”  $\Delta$  of  $\Gamma$  on which it acts by reflection in  $k$  (under relabelling): this is depicted in the blue segment  $AB \dots B'A'$  in either of the two diagrams of Figure 7.

When  $k$  ends in a vertex (e.g.,  $C$  on the right in Figure 7), we have a “fundamental subchain”  $\Delta'$  ( $ABC$  in our example), reflected under  $\rho$  to  $\Delta''$  (i.e.,  $A'B'C$ ), with  $\Delta$  the union of  $\Delta'$  and  $\Delta''$ .

When  $k$  ends in the midpoint of  $\Delta$  of an edge  $CC'$  of  $\Gamma$  (e.g.,  $N_0$  on the left in Figure 7), the “fundamental subchain”  $\Delta'$  ends in  $C$  (so  $\Delta' = ABC$  in our example), and  $\Delta$  is the union of  $\Delta'$ , its reflection  $\Delta''$ , and the middle segment  $CC'$ .

Similarly, the generator  $\sigma$  has a “basic subchain”  $\Theta$  with “fundamental subchain”  $\Theta'$  (given by  $AZYX$  in both diagrams of Figure 7).

**Theorem 6.8.** *Let  $\Gamma$  be a planar  $n$ -polygon and  $H \cong D_{2d}$  is a dihedral subgroup of  $\text{Aut}(\Gamma)$ , generated by reflections in axes  $k$  and  $m$  in a regular  $n$ -gon  $\Gamma_n$ . The fixed-point set  $\tilde{\mathcal{C}} = \tilde{\mathcal{C}}(\Gamma)^H$  splits as a disjoint union indexed by  $\tilde{\mathcal{C}}(\Gamma_d^{\text{eq}})^H$ . For each  $\tilde{\mathbf{z}} \in \tilde{\mathcal{C}}(\Gamma_d^{\text{eq}})^H$ , the corresponding component  $\tilde{\mathcal{C}}_{\tilde{\mathbf{z}}}$  of  $\tilde{\mathcal{C}}$  fibers over an interval  $[0, L_0]$ . The fiber over a value  $L$  (the length of all edges of  $\tilde{\mathbf{z}}$ ) further fibers over a closed interval  $I = I_L$  in the  $\mathbb{R}P^1 \cong S^1$  (the space of lines in the plane through the barycenter  $\tilde{\mathbf{z}}(O)$ ). Finally, given a line  $\tilde{\mathbf{x}}(k)$  in  $I$ , let  $\tilde{\mathbf{x}}(m)$  denote its rotation by an angle of  $\pi/d$  about  $\tilde{\mathbf{z}}(O)$ ; the fiber of  $\tilde{\mathcal{C}}$  over  $\tilde{\mathbf{x}}(k)$  is then isomorphic to  $Y_{\tilde{\mathbf{x}}(k)} \times Y'_{\tilde{\mathbf{x}}(m)}$ .*

**Corollary 6.9.** *For  $\Gamma$ ,  $H = D_{2d}$ , and the two open chains  $\Delta'$  and  $\Theta'$  as above, the interior of  $\tilde{\mathcal{C}}(\Gamma)^H$  has a local parametrization given by  $(0, L_0) \times I \times \tilde{\mathcal{C}}(\Delta') \times \tilde{\mathcal{C}}(\Theta')$ .*

*Proof.* Given any  $L > 0$ , let  $\Gamma_d^{\text{eq}}$  be an equilateral  $d$ -gon with edge length  $L$  and let  $\tilde{\mathbf{z}} \in \tilde{\mathcal{C}}(\Gamma_d^{\text{eq}})^H$  be a fully reduced fully symmetric configuration



for  $\Gamma_d^{\text{eq}}$ . Let  $A'$  and  $A''$  be the first two vertices of the  $d$ -gon (so  $\tilde{\mathbf{z}}(A')$  is at the origin,  $\tilde{\mathbf{z}}(A'')$  is in the positive direction of the  $x$  axis, and  $d(\tilde{\mathbf{z}}(A'), \tilde{\mathbf{z}}(A'')) = L$ ).

In order to determine a fully reduced symmetric configuration  $\tilde{\mathbf{x}}$  for  $\Gamma$  (invariant under relabelling in the given subgroup  $H$ ), we must choose a line  $\tilde{\mathbf{x}}(k)$  through the barycenter  $\tilde{\mathbf{z}}(O)$  of  $\tilde{\mathbf{z}}$ , which will serve as the axis of the *geometric* reflection realizing the action of  $\rho$  by reflecting the *labels* in the “combinatorial axis”  $k$ .

We let  $\tilde{\mathbf{x}}(m)$  be the line through  $\tilde{\mathbf{z}}(O)$  forming an angle of  $\pi/d$  with  $\tilde{\mathbf{x}}(k)$  (realizing geometrically the reflection  $\sigma$  in  $m$ ), and let  $\tilde{\mathbf{x}}(A)$  be the reflection of the origin (which is  $\tilde{\mathbf{z}}(A')$ ) in the geometric axis  $\tilde{\mathbf{x}}(k)$ .

Note that  $\tilde{\mathbf{z}}(O)$  is the center of the circle  $\gamma$  circumscribing the regular  $d$ -gon  $\tilde{\mathbf{z}}$  and  $\tilde{\mathbf{x}}(k)$  bisects  $\angle \tilde{\mathbf{z}}(A')\tilde{\mathbf{z}}(O)\tilde{\mathbf{z}}(A)$ , so  $\tilde{\mathbf{x}}(m)$  bisects  $\angle \tilde{\mathbf{z}}(A'')\tilde{\mathbf{z}}(O)\tilde{\mathbf{z}}(A)$ . Since  $d(\tilde{\mathbf{z}}(O), \tilde{\mathbf{x}}(A)) = d(\tilde{\mathbf{z}}(O), \tilde{\mathbf{z}}(A'))$ ,  $\tilde{\mathbf{x}}(A)$  is also on  $\gamma$ , so  $\tilde{\mathbf{x}}(A)$  is also the reflection of  $\tilde{\mathbf{z}}(A'')$  in  $\tilde{\mathbf{x}}(m)$ .

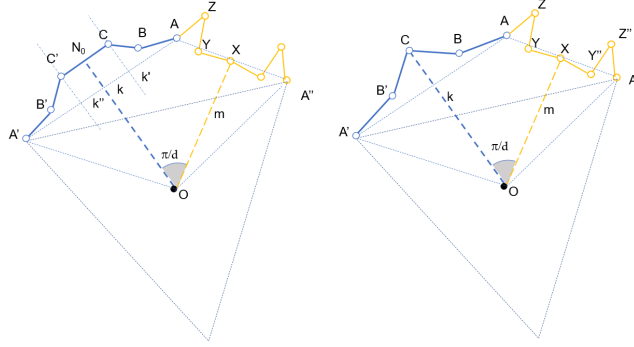


FIGURE 7. Symmetric configurations under double reflections

In this situation, a pair of reduced configurations  $(\hat{\mathbf{u}}, \hat{\mathbf{v}})$  for the open chains  $\Delta'$  and  $\Theta'$ , respectively, generally will determine (up to) four reduced configurations  $\hat{\mathbf{y}}$  for the chain  $\Delta \cup \Theta$  (the blue and yellow in Figure 7), with endpoints  $\hat{\mathbf{y}}(A')$  and  $\hat{\mathbf{y}}(A'')$  (such that  $d(\hat{\mathbf{y}}(A'), \hat{\mathbf{y}}(A'')) = L$ ).

To see how, we must distinguish two basic cases:

- (a) If the original axis  $k$  (for the reflection  $\rho$ ) ends in a vertex  $D$ , as on the right-hand side of in Figure 7, the fundamental open subchain  $\Delta'$  of  $\Gamma$  is  $(A, \dots, C)$ , say. Let  $\lambda(\hat{\mathbf{u}}) = d(\hat{\mathbf{u}}(A), \hat{\mathbf{u}}(C))$  be the length of a reduced configuration  $\hat{\mathbf{u}}$  for  $\Delta'$  (a smooth function on the torus  $\widehat{\mathcal{C}}(\Delta')$ ). The circle  $\gamma_{\hat{\mathbf{u}}}$  of radius  $\hat{\mathbf{u}}(\lambda)$  about  $\tilde{\mathbf{x}}(A)$  generally intersects  $\tilde{\mathbf{x}}(k)$  in two points  $\tilde{\mathbf{x}}'(C)$  and  $\tilde{\mathbf{x}}''(C)$  (which coincide if  $d(\tilde{\mathbf{x}}(A), \tilde{\mathbf{x}}(k)) = \lambda(\hat{\mathbf{u}})$ ). If this happens, we say that the reduced configuration  $\hat{\mathbf{u}}$  of  $\Delta'$  is *allowable* with respect to  $(\tilde{\mathbf{z}}, \tilde{\mathbf{x}}(k))$ .

Allowable configurations  $\hat{\mathbf{v}}$  of  $\Theta'$  are defined similarly if the axis  $m$  for  $\sigma$  ends in a vertex of  $\Gamma$ , when the circle  $\gamma_{\hat{\mathbf{v}}}$  of radius  $\mu(\hat{\mathbf{v}})$  about  $\tilde{\mathbf{x}}(A)$  intersects  $\tilde{\mathbf{x}}(m)$ .

- (b) If  $k$  ends in the midpoint  $N_0$  of an edge of  $\Gamma$  (of length  $\ell_i$ , say), as on the left hand side of in Figure 7, let  $\tilde{\mathbf{x}}(k')$  be the line parallel to  $\tilde{\mathbf{x}}(k)$  at a distance of  $\ell_i/2$  on the same side as  $\tilde{\mathbf{x}}(A)$ . In this case, a reduced configuration  $\hat{\mathbf{u}}$  of  $\Delta'$  of distance  $\lambda(\hat{\mathbf{u}}) = d(\hat{\mathbf{u}}(A), \hat{\mathbf{u}}(D))$  will be *allowable* with respect to  $(\tilde{\mathbf{z}}, \tilde{\mathbf{x}}(k))$  if the circle  $\gamma_{\hat{\mathbf{u}}}$  intersects  $\tilde{\mathbf{x}}(k')$ . Similarly for  $\Theta'$  if the axis  $m$  ends in a midpoint.

A pair of allowable reduced configurations  $(\hat{\mathbf{u}}, \hat{\mathbf{v}})$  for the open chains  $\Delta'$  and  $\Theta'$ , determines a reduced configuration  $\hat{\mathbf{y}}$  for the chain  $\Delta \cup \Theta$ , by letting  $\hat{\mathbf{y}}(C)$  be one of the two intersections of the circle  $\gamma_{\hat{\mathbf{u}}}$  with  $\tilde{\mathbf{x}}(k)$ , and similarly for the endpoint of  $\Theta'$ .

When  $L = 0$ , we think of  $\tilde{\mathbf{z}}$  as the unique infinitesimal fully symmetric configuration for  $\Gamma_d^{\text{eq}}$ . We may then take  $\tilde{\mathbf{x}}(k)$  to be the  $x$ -axis, say. This determines  $\tilde{\mathbf{x}}(m)$ , and of course,  $\tilde{\mathbf{x}}(A)$  will remain at the origin.

Each reduced configuration  $\hat{\mathbf{y}}$  for the chain  $\Delta \cup \Theta$  yields a unique fully reduced configuration  $\tilde{\mathbf{x}}$  in the fixed-point set  $\tilde{\mathcal{C}}(\Gamma)^H$ , by *rotating*  $\hat{\mathbf{y}}$  about  $\tilde{\mathbf{z}}$ , since by comparing angles, we see that the continuation of  $\tilde{\mathbf{x}}(k)$  beyond  $\tilde{\mathbf{z}}(O)$  is a rotation of  $\tilde{\mathbf{x}}(m)$ , and conversely. See Figure 8.

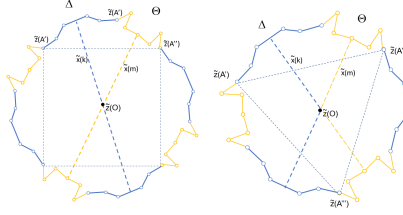


FIGURE 8. Fully symmetric configurations under double reflections

Let  $\Gamma_d^{\text{eq}}$  be an equilateral  $d$ -gon with edge length  $L$  and let  $\tilde{\mathbf{z}} \in \tilde{\mathcal{C}}(\Gamma_d^{\text{eq}})^H$  be a fully reduced fully symmetric configuration for  $\Gamma_d^{\text{eq}}$ , as above.

Each line  $\tilde{\mathbf{x}}(k)$  through  $\tilde{\mathbf{z}}(O)$  determines a subspace  $Y_{\tilde{\mathbf{x}}(k)}$  of the pointed configuration space  $\mathcal{C}_*(\Delta')$  (a torus), consisting of all configurations  $\mathbf{u}$  for  $\Delta'$  (starting at the origin) whose end-point  $\mathbf{u}(C)$  lies on

$$\begin{cases} \tilde{\mathbf{x}}(k) & \text{when } \Delta' \text{ has an even number of edges} \\ \tilde{\mathbf{x}}(k'') & \text{when } \Delta' \text{ has an odd number of edges} \end{cases}$$

See the right and left diagrams in Figure 7, respectively.

We let  $\tilde{\mathbf{x}}(m)$  be the line through  $\tilde{\mathbf{z}}(O)$  forming an angle of  $\pi/d$  with  $\tilde{\mathbf{x}}(k)$ , and the subspace  $Y'_{\tilde{\mathbf{x}}(m)}$  of  $\mathcal{C}_*(\Theta')$  is defined analogously, with  $\tilde{\mathbf{x}}(m)$  replacing  $\tilde{\mathbf{x}}(k)$ .

To identify these subspaces, let  $\mu = \mu(\tilde{\mathbf{x}}(k))$  denote the distance of the origin  $\tilde{\mathbf{z}}(A')$  from  $\tilde{\mathbf{x}}(k)$ , and let  $\mu_{\vec{\ell}} := \ell_1 + \dots + \ell_j$ , where  $\vec{\ell} = (\ell_1, \dots, \ell_j)$  be the length vector of  $\Delta'$ :

- (i) If  $\mu > \mu_{\vec{\ell}}$ , clearly  $Y_{\tilde{\mathbf{x}}(k)} = \emptyset$ .
- (ii)  $\mu = \mu_{\vec{\ell}}$ , then  $Y_{\tilde{\mathbf{x}}(k)}$  consists of a single point: the fully stretched configuration.
- (iii) If  $0 < \mu < \mu_{\vec{\ell}}$ , we see that  $Y_{\tilde{\mathbf{x}}(k)}$  is isomorphic to the disjoint union of two copies of the reduced configuration space  $\widehat{\mathcal{C}}(\widehat{\Delta}')$ , where  $\widehat{\Delta}'$  is the *closed* chain having length vector  $\widehat{\vec{\ell}} = (\ell_1, \dots, \ell_j, \mu)$ : this is because for each reduced configuration  $\widehat{\mathbf{w}} \in \widehat{\mathcal{C}}(\widehat{\Delta}')$ , we obtain two reduced configurations  $\widehat{\mathbf{u}}_1, \widehat{\mathbf{u}}_2 \in \widehat{\mathcal{C}}(\widehat{\Delta}')$  by rotating  $\widehat{\mathbf{w}}$  about the origin so that the endpoint  $\widehat{\mathbf{w}}(C)$  of  $\Delta'$  lies at one of the two intersections of the circle of radius  $\mu$  about the origin with  $\tilde{\mathbf{x}}(k)$ .
- (iv) If  $\mu = 0$  – that is,  $\tilde{\mathbf{x}}(k)$  passes through the origin –  $Y_{\tilde{\mathbf{x}}(k)}$  decomposes into two complementary subspaces:
  1.  $Y_0$ , consisting of those configurations  $\widehat{\mathbf{u}} \in \mathcal{C}_*(\Delta')$  for which  $\mathbf{u}(C)$  is at the origin. This may be identified with pointed configurations for the closed chain  $\Gamma_j^{\text{cl}}$  with length vector  $\vec{\ell}$ , so  $Y_0 \cong \widetilde{\mathcal{C}}(\Gamma_j^{\text{cl}}) \times S^1$ , where the parameter  $\phi \in S^1$  determines the rotation of the reduced configuration  $\widehat{\mathbf{u}} \in \widetilde{\mathcal{C}}(\Gamma_j^{\text{cl}})$  about the origin (see §4.1).
  2.  $Y_1$ , consisting of pointed configurations  $\widehat{\mathbf{u}} \in \mathcal{C}_*(\Delta')$  not ending at the origin. These are again determined by rotating any reduced configuration  $\widehat{\mathbf{u}}$  for  $\Delta'$  about the origin, till its endpoint lies on one of the two intersections of the circle of radius  $\lambda(\widehat{\mathbf{u}})$  about the origin with the line  $\tilde{\mathbf{x}}(k)$ .

Note that  $\mathcal{C}_*(\Delta')$  is canonically isomorphic to  $\widetilde{\mathcal{C}}(\Delta') \times S^1$  (see §2.1), which explains how both  $Y_0$  and  $Y_1$  embed in  $\mathcal{C}_*(\Delta')$ .

We see that given  $(\tilde{\mathbf{z}}, L)$  as above, the pair of configurations  $(\widehat{\mathbf{u}}, \widehat{\mathbf{v}})$  for  $\Delta'$  and  $\Theta'$ , respectively, is allowable if and only if  $\widehat{\mathbf{u}} \in Y_{\tilde{\mathbf{x}}(k)}$  and  $\widehat{\mathbf{v}} \in Y'_{\tilde{\mathbf{x}}(m)}$ . Note that the maximal value of  $L$  for which such allowable pairs exist is  $L = L_0 := 2\mu_{\vec{\ell}} + 2\mu'_{\vec{\ell}'} + \nu$ , where  $\nu$  is the sum of the lengths of the middle edges of  $\Delta$  and  $\Theta$  (if these have an odd number of edges, as in the right picture in Figure 8). In this case, there is a unique allowable pair, yielding a fully stretched configuration for  $\Delta \cup \Theta$ .  $\square$

## 7. Triangulating a cell for the hexagon

As noted in Remark 6.2, a full  $\text{Aut}(\Gamma)$ -equivariant cell structure for the fully reduced configuration space  $\widetilde{\mathcal{C}}(\Gamma)$  of a polygon  $\Gamma$  requires a refinement of the regular cell structure of Section 5. We illustrate some of the issues involved by considering a single regular cell  $E = E_{\text{Id}}$  of strictly convex configurations for

the equilateral hexagon  $\Gamma = \Gamma_6^{\text{eq}}$ . Note that  $E$  itself is a bipyramid with six triangular facets, as in Figure 9 (in which the outer edges are to be identified pairwise as indicated).

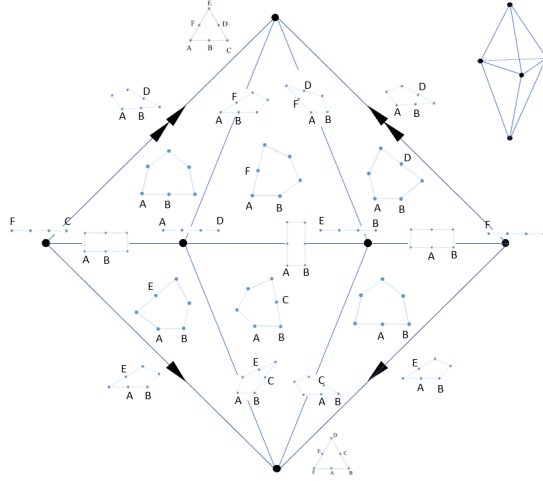


FIGURE 9. Bipyramid for the equilateral hexagon

*Remark 7.1.* The vertices of  $\tilde{\mathcal{C}}(\Gamma)$  are determined by a combination of symmetries and straightenings or foldings, which suffice to determine a rigid configuration. The full list of all vertices for the equilateral hexagon in the regular cell structure of Section 5 are of eleven types, depicted in Figure 10 (although, as we see in Figure 9, the same type may appear with different labellings).

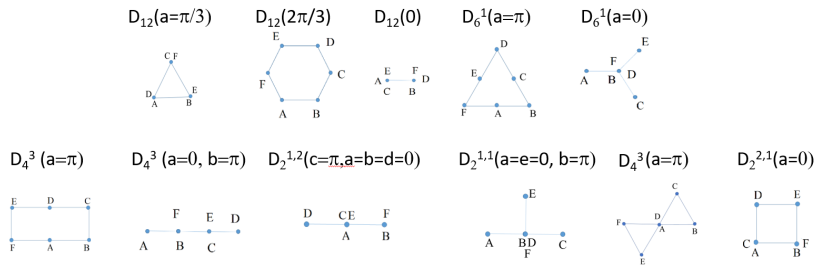


FIGURE 10. The vertex types of  $\tilde{\mathcal{C}}(\Gamma)$  for the equilateral hexagon

**7.1. The subdivided bipyramid**

The bipyramid  $E = E_{\text{Id}}$  of (strictly) convex configurations for the equilateral hexagon  $\Gamma = \Gamma_6^{\text{eq}}$ , should be subdivided into twelve tetrahedra, which are permuted among themselves by action of  $\text{Aut}(\Gamma)$  on the labels. In accordance with the principles of §5.2, each tetrahedron is determined by specifying the largest of the six angles of  $\Gamma$ , and then choosing which of the two angles adjacent to it should be smaller.

This in Figure 11 (on the left) we have required that the angle  $\theta_B$  (labelled by  $B$ ) should be the greatest, and that  $\theta_A < \theta_C$ . One can then determine the induced inequalities  $\theta_A < \theta_D < \theta_F$ , and  $\theta_C < \theta_E, \theta_F$ , as indicated in the lower left corner of Figure 11.

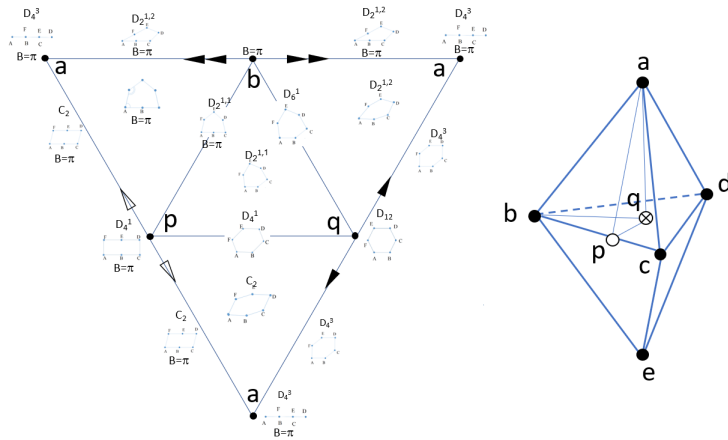


FIGURE 11. Fine 3-cell for the equilateral hexagon  $\Gamma = \Gamma_6^{\text{eq}}$  (one of twelve)

The boundary of the tetrahedron  $abpq$  consist of four triangular facets:

- (a) The boundary triangle  $\triangle abp$  is determined by the requirement that  $\theta_B = \pi$  (a straightening, which we abbreviate to  $B = \pi$  in the figure), so it is an open cell of the fully-reduced configuration space of the pentagon with length vector  $\vec{\ell} = (2, 1, 1, 1, 1)$ . In turn its boundary consists of:
  - i. The edge  $ab$ , corresponding to the further straightening  $F = \pi$ , yields a deltoid of sides  $\{2, 1\}$  and symmetry group  $C_2$  (corresponding to the subgroup  $D_2^{1,2}$  of  $\text{Aut}(\Gamma) = D_{12}$  in Figure 3, generated by the reflection in the diagonal  $BE$  of the hexagon).

- ii. The edge  $ap$ , corresponding to the straightening  $E = \pi$  yields a parallelogram of sides  $\{2, 1\}$  and symmetry group  $C_2$  (corresponding to the subgroup  $C_2 < D_{12}$  generated by the rotation by  $180^\circ$ ).
- iii. The edge  $bp$ , corresponding to the symmetric version of the  $(2, 1, 1, 1, 1)$ -pentagon, with  $C_1$ -symmetry corresponding to  $D_2^{1,1} < D_{12}$ .
- (b) The central triangle  $\triangle bpq$  in Figure 11 is determined by requiring invariance under the subgroup  $D_2^{1,1}$  mentioned above.
- (c) The upper right triangle  $\triangle abq$  is invariant under the subgroup  $D_2^{1,2}$  (generated by reflection in the diagonal  $AD$ ), so the common edge with the central triangle has symmetry group  $D_6^1$  (generated by the two reflections and thus including the rotation by  $120^\circ$ ).
- (d) The bottom triangle  $\triangle apq$  is invariant under the subgroup  $C_2$  (generated by the  $180^\circ$  rotation). The edge  $pq$  consists of configurations invariant under the subgroup  $D_6^1$  of  $D_{12}$  generated by the reflections in  $BF$  and the median connecting the midpoints of  $AF$  and  $CD$ .

*Remark 7.2.* As noted above, the tetrahedron on the left of Figure 11 appears as one of twelve subcells in the bipyramid of Figure 9, obtained by a barycentric subdivision as on the right in Figure 11: specifically, the upper left facet labelled  $B = \pi$  in Figure 11 is one half of the upper left facet of Figure 9, ending at the center of the lower edge of the latter (the vertex corresponding to the rectangle marked  $B = \pi$  and  $D_4^1$  in the former). The vertex marked  $D_{12}$  in the tetrahedron is the barycenter  $q$  of the bipyramid in Figure 11, corresponding to the regular hexagon configuration. Observe that all other facets of the tetrahedron are symmetric – that is, fixed under an appropriate subgroup of  $\text{Aut}(\Gamma)$ , as indicated in Figure 11 – and are thus internal membranes of the bipyramid, in the language of §5.2.

## 8. The equilateral pentagon

We now analyze in detail the case of the equilateral pentagon  $\Gamma_5^{\text{eq}}$ . Recall that [Hav, §2.4] identifies the reduced configuration space of  $\Gamma_5^{\text{eq}}$  (that is,  $\widehat{\mathcal{C}}(\Gamma_5^{\text{eq}})$  modulo orientation-preserving isometries) as a genus 4 oriented surface (see also [KM]), while [K] shows that the fully reduced configuration space  $\mathcal{C}(\Gamma_5^{\text{eq}})$  of §2.1 is the connected sum of five projective planes. Note that Remark 2.3 applies in this case.

### 8.1. Cells for the pentagon

An analysis of the possible arrow diagrams for an equilateral pentagon shows that there are only four dihedral types: the first, third, fourth, and fifth in Figure 12. Note that the first and second have the same dihedral type, but different

cyclic types (with reversed orientations), as we see from the corresponding configurations (which are equivalent in the fully reduced configuration space  $\tilde{\mathcal{C}}(\Gamma)$ , but not in  $\hat{\mathcal{C}}(\Gamma)$ ). The fourth and sixth also have the same dihedral types, but distinct cyclic types.

In order to get a better grasp of the fine cell structure, it is convenient to use here a slightly different labelling system, corresponding to open intervals of allowable values for each of the five angles between consecutive edges (as in §3.1). We indicate the range  $0 < \theta < \pi$  by  $-$ , and  $\pi < \theta < 2\pi$  by  $+$  (using the convention of §3.4). Each sequence of the form  $(+ + - - -)$ , for example, defines a unique cell, except for  $(- - - - -)$ , which corresponds to two distinct cells as indicated in Figure 12 (where all five types are shown). The cell marked  $(- - - - -)$  has smallest angle  $\geq 2 \arcsin(0.25) \approx 0.5053$ , while the cell marked  $(- - - - -)'$  has largest angle  $\leq \pi/3$  (with dual conditions for  $(+ + + + +)$  and  $(+ + + + +)'$ ).

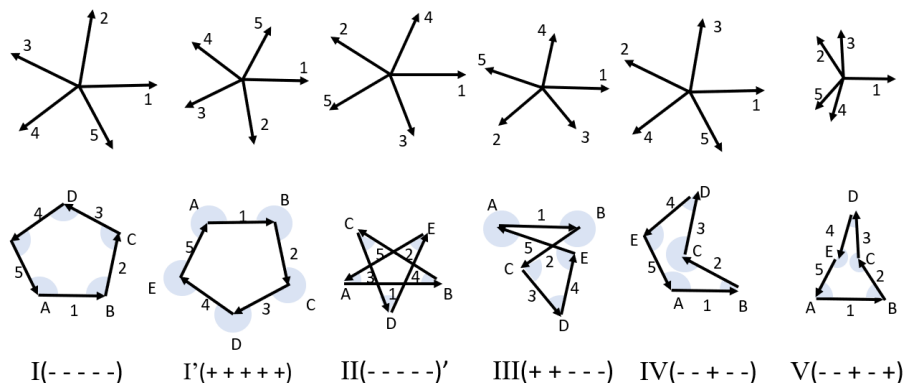


FIGURE 12. Cells for pentagon

Note that switching all signs corresponds to reversing the cyclic order, while a cyclic shift in the sequence corresponds to a cyclic shift in the labelling. Thus (in the order in which they appear from left to right in Figure 12) we have:

- I. One (pentagonal-shaped) cell for the convex pentagon  $(- - - - -)$  (as in Figure 14 below);
  - I'. An analogous (pentagonal-shaped) cell for the convex pentagon  $(+ + + + +)$ ;
  - II. One (pentagonal-shaped) cell for each of the pentagrams  $(- - - - -)'$  and  $(+ + + + +)'$ ;
  - III. Five (hexagonal-shaped) cells:  $(+ + - - -)$ ,  $(+ + - - -)$ ,  $(- + + - -)$ ,  $(- - + + -)$ , and  $(- - - + +)$ , for the middle type, as in Figure 16 below).
- Similarly, we have five (hexagonal-shaped) cells for the reverse order (which looks identical if we disregard the direction in which the angles are measured).
- IV. Five (hexagonal-shaped) cells of type  $(+ - - - -)$ , et cetera (see Figure 13)

V. Five triangular cells of type  $(++-+-)$ , et cetera (see Figure 17 below).

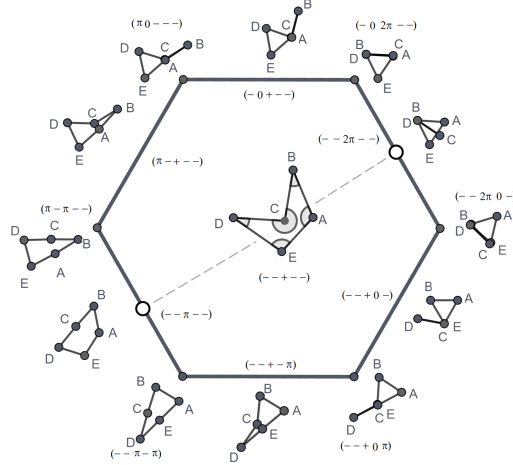


FIGURE 13. Cell  $(- - + - -)$

## 8.2. Boundaries of the cells

As noted above, one should think of the 32 cells constituting the reduced configuration space for the equilateral pentagon as polygonal cells (triangles, pentagons, or hexagons), identified along common edges. The edges of each such polygonal cell are obtained by a collineation: either straightening one of the angles to  $\pi$ , or folding it to 0 (if it was a  $-$ ) or  $2\pi$  (if it was a  $+$ ). Each vertex  $P$  of a cell is obtained by a double collineation, corresponding to the two edges meeting at  $P$ .

It is possible to describe explicitly the rules for the allowable collineations and double collineations (for example, one cannot have two adjacent straightenings), but as these are particular to the case  $n = 5$ , we leave them to the reader, illustrating them in Figures 13, 17, 16, and 14.

## 8.3. Symmetries of the equilateral pentagon

Each of the five types of cells corresponding to the configurations in Figure 12 are exchanged among themselves by the obvious cyclic rotations or reflections of the vertices, so only one of each type is needed for the fundamental domain of the symmetric configuration space. However, there are also symmetries acting on each cell. For example, the dashed line across the hexagon in Figure 13 represents an axis of symmetry, and indeed the two halves of the hexagon are exchanged under the reflection fixing  $C$ , with  $A \leftrightarrow E$  and  $B \leftrightarrow D$ . The upper left half of the hexagon corresponds to the linear ordering of the angles



$\gamma > \alpha > \varepsilon > \delta > \beta$ , while the lower right half corresponds to  $\gamma > \alpha > \varepsilon > \beta > \delta$ ,

The cell for  $(- - - - -)$  is a pentagon, but in this case there is a tenfold symmetry – as shown in Figure 14. Here each triangular slice of the pentagonal cell corresponds to a certain linear ordering of the angles of our equilateral pentagon  $\Gamma = \Gamma_5^{\text{eq}}$  (shown on the right of Figure 14). Each triangular section has one vertex at the center of the cell (the regular pentagon configuration), one at a vertex of cell (corresponding to two collineations), and one at the unique (isosceles) trapezoid configuration with one collineation, which is the midpoint of an edge. The dashed sides of each slice are obtained by changing one inequality to an equality. Compare to the subdivided bipyramid on the right in Figure 11.

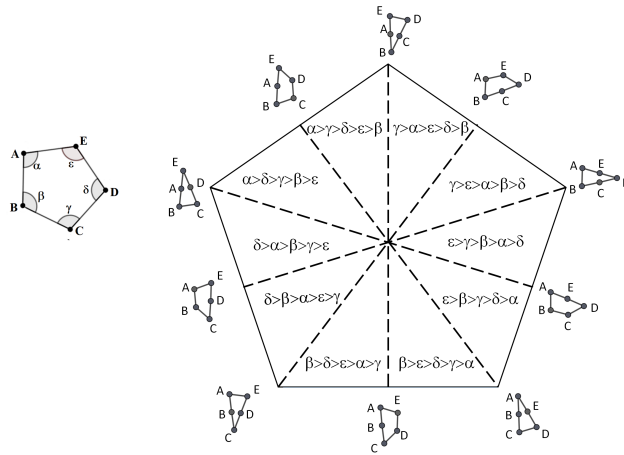


FIGURE 14. Symmetries of the cell for  $(- - - - -)$

The cell for  $(- - - - -)'$  (second from the left in Figure 12) is also a pentagon, similarly divided into 10 triangular regions, as shown in Figure 15.

The cell for  $(+ + - - -)$  (third from the left) is pentagonal, divided into two halves (see Figure 16), but with the bisector connecting a vertex to the midpoint of the edge opposite.

The cell for  $(+ + - + -)$  (on the right) is a triangle, similarly subdivided into two halves, as in Figure 17.

#### 8.4. The symmetric configuration space of the pentagon

From the above discussion we see that a fundamental domain  $\mathcal{F}$  for the action of  $\text{Aut}(\Gamma_5)$  on the reduced configuration space  $\widehat{\mathcal{C}}(\Gamma_5)$ , depicted in Figure 18, is the union of:

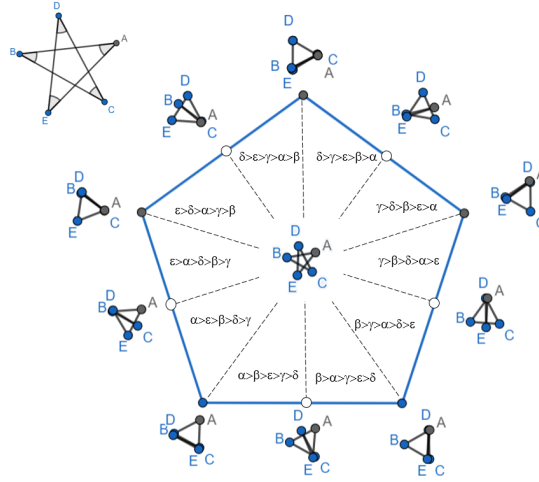


FIGURE 15. The cell for  $(-----)'$

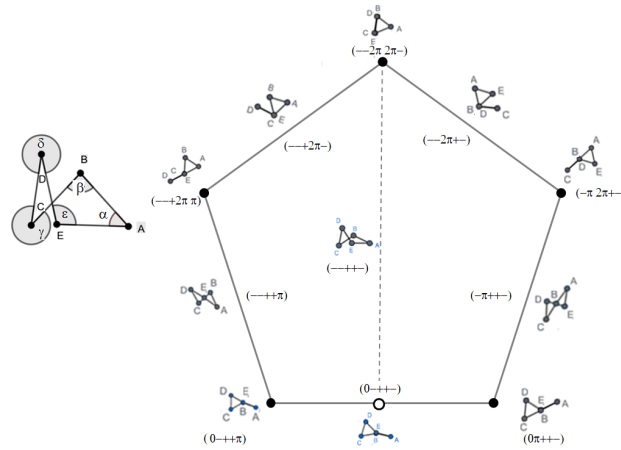


FIGURE 16. The cell for  $(---++-)$

- (i) One half of the hexagonal cell for  $(---+--)$  of Figure 13, marked IV.
- (ii) Attached to it along a half-edge we have one tenth of the pentagonal cell for  $(-----)$  of Figure 14, marked I.
- (iii) Along the opposite half-edge we have another tenth of the analogous pentagonal cell for  $(-----)'$ , marked II.

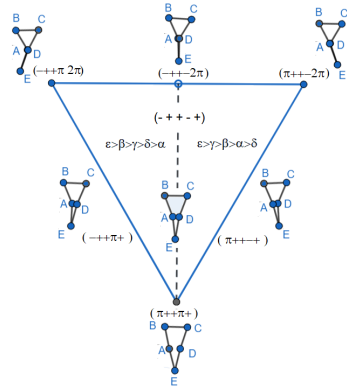


FIGURE 17. The cell for  $(- + + - +)$

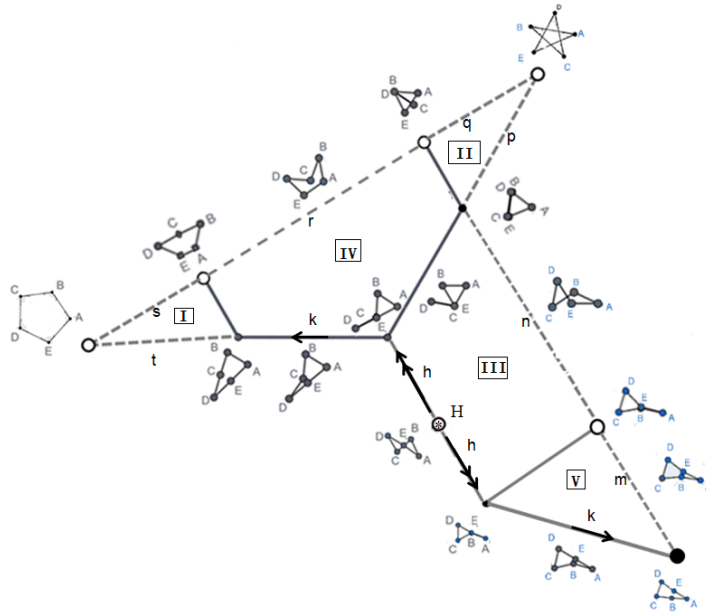


FIGURE 18. Fundamental domain for pentagon

- (iv) One full edge of the cell IV is glued to an edge of the half-pentagonal cell III for  $(- + + - -)$  of Figure 16.
- (v) Finally, the half-cell III for  $(- + + - -)$  is glued along a half-edge to one half V of the triangle for  $(- + + - +)$  of Figure 17.

The boundary of the fundamental domain  $\mathcal{F}$  consists of two types of segments

- a. The two copies of each of the solid edges  $h$  and  $k$  are identified pairwise under appropriate symmetries. The point marked  $H$  is fixed under the symmetries.
- b. Each of the dashed lines  $m, n, p, q, r, s$  and  $t$  is an original axis of symmetry in Figures 13, 17, 16, and 14, respectively, so they are also fixed under the corresponding symmetries, with points on the other side (in the full cell) reflected back into  $\mathcal{F}$ .

Thus we may summarize the results of this section in:

**Proposition 8.1.** *The fully reduced symmetric configuration space  $\widetilde{\mathcal{SC}}(\Gamma_5^{\text{eq}})$  of the equilateral pentagon in the plane is homeomorphic to a closed disc.*

*Proof.* The fundamental domain  $X$  in Figure 18 is a subspace of the fully reduced configuration space  $\widetilde{\mathcal{C}}(\Gamma_5^{\text{eq}})$ , with  $i : X \rightarrow \widetilde{\mathcal{C}}(\Gamma_5^{\text{eq}})$  the inclusion. If  $p : \widetilde{\mathcal{C}}(\Gamma_5^{\text{eq}}) \rightarrow \widetilde{\mathcal{SC}}(\Gamma_5^{\text{eq}})$  is the quotient map, we see that  $p \circ i : X \rightarrow \widetilde{\mathcal{SC}}(\Gamma_5^{\text{eq}})$  is surjective, and one-to-one except along the intervals marked  $h$  and  $k$  in Figure 18. Thus if  $r : X \rightarrow \widehat{X}$  is the quotient map identifying the two copies of  $h$  and  $k$  respectively, we see that  $p \circ i$  induces a homeomorphism  $\varphi : \widehat{X} \rightarrow \widetilde{\mathcal{SC}}(\Gamma_5^{\text{eq}})$  (since the closed disc  $\widehat{X}$  is compact).  $\square$

## Appendix A. Configuration spaces for quadrilaterals

As noted above, the usual configuration spaces of planar quadrilaterals are well known (see, e.g., [F2, §1]). However, we need their detailed description in order to analyze the symmetric configuration spaces. Thus, in this Appendix we prove Theorem 3.3 by considering separately the six cases of §3.5:

**I.** The isosceles quadrilateral case:

When  $\Gamma = ABCD$  is a quadrilateral in the plane with opposite edges  $AB$  and  $CD$  of equal length, we may parameterize the configurations  $\mathbf{x}$  of  $\Gamma$  as in §3.4 by a subset of the angles at the four vertices, by choosing  $\angle BAD$  (from  $\vec{AD}$  to  $\vec{AB}$ ), and  $\angle CDA$  (from  $\vec{DC}$  to  $\vec{DA}$ , both measured counter clockwise). We think of  $\phi := \angle BAD$  as the basic continuous parameter, and note that to each value of  $\phi$  we associate two values of  $\angle CDA$ , corresponding to the elbow up/down position of  $C$   $\varepsilon = \pm 1$  (in §3.4) – see Figure 19. Note that the precise rule for calculating  $\phi'$  and  $\phi''$  from  $\phi$  is complicated to state.

We need to understand the action of the  $C_2$ -symmetry of  $\mathcal{T}^\Gamma$  (generated by the graph automorphism  $f : \mathcal{T}^\Gamma \rightarrow \mathcal{T}^\Gamma$  given by  $A \leftrightarrow D$  and  $B \leftrightarrow C$  on a configuration  $\mathbf{x} \in \widehat{\mathcal{C}}(\Gamma)$ ). In the language of §2.4, our permutation  $\sigma$  is given by  $\begin{pmatrix} 1234 \\ 4321 \end{pmatrix}$ , which reverses cyclic orientation, so  $\mathbf{x} = (\phi, \alpha, \beta, \phi')$  maps under  $f$  to  $\mathbf{y} = N(\widehat{\mathbf{x}} \circ f) = (2\pi - \phi', 2\pi - \beta, 2\pi - \alpha, 2\pi - \phi)$  (where  $\alpha$  and  $\beta$  are extraneous to determining the configuration, and may therefore be dropped).

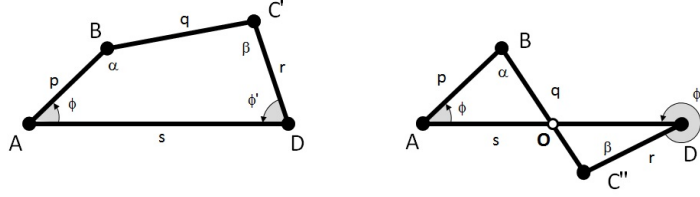


FIGURE 19. Parameterizing a quadrilateral

Thus the action of  $C_2 = \text{Aut}(\Gamma)$  on  $\widehat{\mathcal{C}}(\Gamma)$  takes  $(\phi, \phi')$ , to  $(2\pi - \phi', 2\pi - \phi)$  as in Figure 20, with fixed points when  $\phi + \phi' = 2\pi$ .

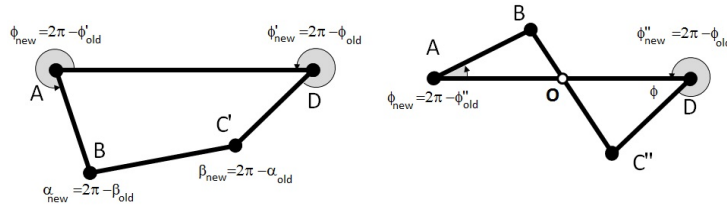


FIGURE 20. Action of  $C_2$  on Figure 19

Case 3.5(i) when  $\Gamma$  is isosceles then may be described as follows:

**Lemma A.1.** *In the notation of §3.2, assume that  $s > p, q, r$ ,  $p = r$ ,  $s < p + q + r$ , and  $s + q > 2p$ . Then  $\widehat{\mathcal{C}}(\Gamma)$  is a circle, the  $C_2$ -action is the reflection in the diameter (with two fixed points), and thus  $\widehat{\mathcal{S}\mathcal{C}}(\Gamma)$  is homeomorphic to a closed interval.*

*Proof.* Consider the circle  $\gamma_B$  of radius  $p = r$  about a fixed point  $A$  in the plane, and another circle  $\gamma_C$  of the same radius about a fixed point  $D$  at distance  $\ell_1$  from  $A$ . These are the loci of allowable locations for  $B$  and  $C$ , respectively, if we disregard the requirement that the distance between them is  $q$ . By the analysis of [MT] (see also [F2, §1]), the reduced configuration space  $\widehat{\mathcal{C}}(\Gamma)$  can be described as follows in our case:

There is an arc  $\zeta$  of the circle  $\gamma_B$  defined as the intersection of  $\gamma_B$  with an annulus  $T$  about  $D$ , where  $T$  consists of the allowable locations for  $B$  with respect to  $\gamma_C$ . Thus the points of  $\zeta$  are precisely the possible locations for  $B$  satisfying all our constraints.

For each point  $B$  of  $\zeta$ , the circle  $\delta$  of radius  $q$  about  $B$  generically intersects  $\gamma_C$  in two points  $C'$  and  $C''$ , corresponding to the elbow up and elbow down positions of  $\angle BCD$  (except for the two endpoints  $B_+$  and  $B_-$  of  $\zeta$ , for which  $C' = C''$  and  $\beta = \angle BCD$  is flat). The angle  $\angle BAD$  is our parameter  $\phi$ , with  $\phi' = \angle C'DA$  and  $\phi'' = \angle C''DA$ .



$C_2$ -action switches the two circles between them (fixing the common point), and thus  $\widehat{SC}(\Gamma)$  is homeomorphic to a circle.

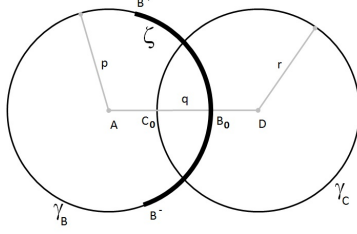


FIGURE 22. Configuration space for isosceles quadrilateral in case (ii)

*Proof.* In Figure 22 the circle  $\delta$  of radius  $q$  about the midpoint  $B_0$  of the arc  $\zeta$  now intersects  $\gamma_C$  in a single point  $C_0$  (which also holds for its endpoints  $B^+$  and  $B^-$ , as before). The fully aligned degenerate trapezoid  $AB_0C_0D$  is fixed by the  $C_2$ -action. Moreover, we see that the non-convex parallelograms corresponding to the fixed points described in the proof of Lemma A.1 are both identified with this degenerate trapezoid, since we have  $AO = \frac{s}{2}$  and  $BO = \frac{q}{2}$  on the right in Figure 19, and their sum equals  $AB = p$  by our assumption.

The argument in the proof of Lemma A.1 shows that the two circles corresponding to the sub-arcs  $B^+B_0$  and  $B^-B_0$  of  $\zeta$  are exchanged under the  $C_2$ -action.  $\square$

**III.** Case 3.5(iii) becomes:

**Lemma A.3.** *In the notation of §3.2, assume that  $s > p, q, r$ ,  $p = r$ ,  $s < p + q + r$ , and  $s + q < 2p$ . Then  $\widehat{C}(\Gamma)$  is a disjoint union of two circles, the  $C_2$ -action switches the two circles between them, and thus  $\widehat{SC}(\Gamma)$  is homeomorphic to a circle.*

*Proof.* In this case the  $\zeta$  of Figures 21-22 splits into two disjoint arcs  $\zeta^+ = B^+B_0^+$  and  $\zeta^- = B^-B_0^-$ , as in Figure 23, and the proof of Lemma A.2 shows that the non-convex parallelogram corresponding to a possible fixed point of the  $C_2$ -action cannot exist. This action simply switches the two disjoint circles of  $\widehat{C}(\Gamma)$  between them, as before.  $\square$

**IV.** Case 3.5(iv) is similar:

**Lemma A.4.** *If  $s = q \geq p > r$  in the notation of §3.2,  $\widehat{C}(\Gamma)$  is a disjoint union of two circles, the  $C_2$ -action switches them, and  $\widehat{SC}(\Gamma)$  is again a circle.*

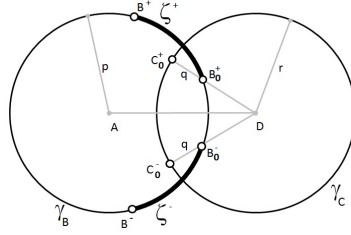


FIGURE 23. Configuration space for isosceles quadrilateral in case (iii)

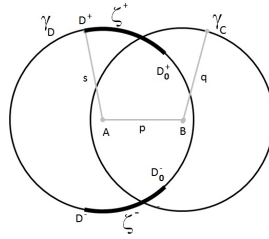


FIGURE 24. Configuration space for isosceles quadrilateral in case (iv)

*Proof.* In Figure 24 we choose to draw the two congruent circles  $\gamma_C$  and  $\gamma_D$  about  $A$  and  $B$ , so that  $\zeta$  again splits into two disjoint arcs  $\zeta^+ = D^+D_0^+$  and  $\zeta^- = D^-D_0^-$ , as in Figure 23, and once more a non-convex parallelogram corresponding to a possible fixed point of the  $C_2$ -action cannot exist. This action again switches the two disjoint circles of  $\widehat{\mathcal{C}}(\Gamma)$  between them.  $\square$

**V.** The case of a parallelogram:

When  $\Gamma = ABCD$  is a parallelogram, the description of **IV** should be modified as follows: specializing the description of Figure 19 as in Figure 25

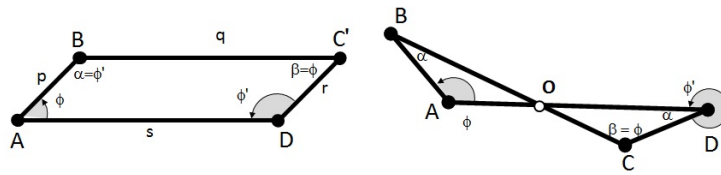


FIGURE 25. Parameterizing a parallelogram

we now have a  $C_2^{(1)} \times C_2^{(2)}$ -symmetry generated by two graph automorphisms: the first  $C_2$ -action is given by  $A \leftrightarrow D$  and  $B \leftrightarrow C$ , and the second by



$A \leftrightarrow B$  and  $C \leftrightarrow D$ . It turns out that the first two coincide on the left (convex) configuration of Figure 25, yielding the left hand side of Figure 26. On the other hand, the first  $C_2$ -action on the right (non-convex) configuration in Figure 25 yields the upper right hand in Figure 26, while the second yields the lower right hand quadrilateral there.

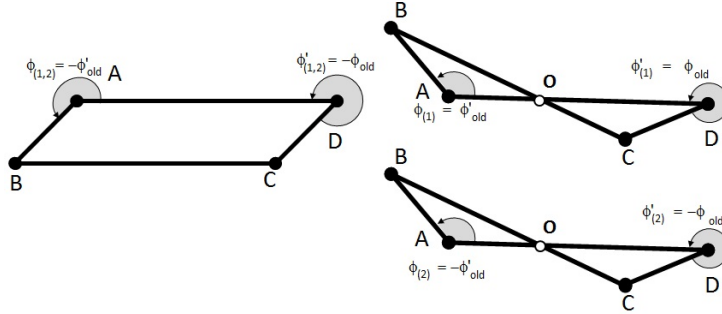


FIGURE 26. Action of  $C_2 \times C_2$  on Figure 25

**Lemma A.5.** *If in the notation of §3.2  $s = q > p = r$  (a parallelogram), then  $\widehat{\mathcal{C}}(\Gamma)$  is a union of four arcs  $x, y, z,$  and  $w$  with ends glued at  $G$  and  $H$ , respectively, as depicted in Figure 27. The first  $C_2$ -action sends  $z$  antipodally to  $w$ , while the second  $C_2$ -action reflects the left half  $x_1$  of  $x$  to the right half  $x_2$  (with a fixed point at their common end  $J$ ), and reflects the left half  $y_1$  of  $y$  to the right half  $y_2$  (with a fixed point at their common end  $K$ ), thus identifying  $G$  with  $H$ . As a result,  $\widehat{\mathcal{S}\mathcal{C}}(\Gamma)$  is a wedge of the circle  $w \sim z$  and a segment.*

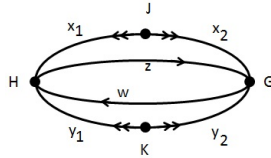


FIGURE 27. Configuration space for the parallelogram of case (v)

*Proof.* In Figure 21 we see that  $\zeta$  equals the whole circle  $\gamma_B$ , and at the two points of intersection of  $\zeta$  with the  $x$ -axis (corresponding to  $G$  and  $H$  in Figure 27) we have  $C' = C''$ , which yields the description of  $\widehat{\mathcal{C}}(\Gamma)$ . The actions of the two cyclic groups  $C_2^{(1)}$  and  $C_2^{(2)}$  follow from the description in Case V.  $\square$

**Lemma A.6.** *If in the notation of §3.2  $s = p > q = r$  (a deltoid) then  $\widehat{\mathcal{C}}(\Gamma)$  is a union of four arcs  $x, y, z,$  and  $w$  with ends glued at  $G$  and  $H$ , respectively, as depicted in Figure 28, with the  $\text{Aut}(\Gamma) = C_2$ -action fixing the arcs  $x$  and  $y$  pointwise and reflecting the arc  $z$  and  $w$  to each other in the diameter  $GH$ . Thus  $\widehat{\mathcal{S}\mathcal{C}}(\Gamma)$  consists of three arcs with left endpoints glued at  $H$  and the right endpoints glued at  $G$ .*

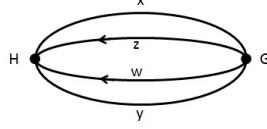


FIGURE 28. Configuration space for the parallelogram of case (v)

*Proof.* The analysis of Lemma A.1 shows that we have an arc  $\zeta$  of the circle  $\gamma_B$  with a single corresponding point  $C' = C''$  on  $\gamma_C$  for its two endpoints  $B^+$  and  $B^-$ , and otherwise two distinct values. These yield the two arcs  $w$  and  $z$  with the  $C_2$ -action as described. However, the fact that  $s = p$  implies that  $\zeta$  passes through  $D$ , at which point the edges  $AB$  and  $AD$  coincide, so  $BC$  and  $CD$  coincide, too, and this common edge is free to rotate about  $D$ , yielding the arcs  $x$  and  $y$ .  $\square$

**VI.** The square:

Recall that if  $\Gamma = \Gamma_4^{\text{eq}}$  is an equilateral quadrilateral, the automorphism group  $\text{Aut}(\Gamma)$  is the dihedral group  $D_4$  generated by the rotation  $R$  (given by  $A \mapsto B, B \mapsto C, C \mapsto D,$  and  $D \mapsto A$ ), of order 4, and the reflection  $T$  (given by  $A \leftrightarrow C$  with  $B$  and  $D$  fixed).

**Lemma A.7.** *In the equilateral case ( $s = p = q = r$ ),  $\widehat{\mathcal{C}}(\Gamma)$  is a union of three circles of four arcs  $x, y, z,$  and  $w$  with ends glued at  $G, H,$  and  $L$ , as depicted in Figure 29. The reflection  $T$  sends  $x$  to  $y, x'$  to  $y', u$  to  $v,$  and fixes  $z$  and  $w$  pointwise. The rotation  $R$  sends  $x$  to  $x', y$  to  $y', u$  to  $z, z$  to  $v, v$  to  $w$  and  $w$  to  $y,$  and fixes  $J, K$  and  $L$ . Thus  $\widehat{\mathcal{S}\mathcal{C}}(\Gamma)$  consists of two arcs corresponding to  $x$  and  $z,$  glued at their common endpoint  $H$ .*

*Proof.* The analysis of Lemma A.1 shows that we have two circles  $\gamma_B$  and  $\gamma_C$  with the same radius  $\ell$  about  $A$  and  $D$  respectively, with  $|AD| = \ell$ . To a point  $B$  on  $\gamma_B$  (with  $\angle DAB = \phi$  as parameter) there correspond two points on  $\gamma_C$ : one being  $A$  itself (so forming a degenerate quadrilateral) and the other,  $C$ , forming a parallelogram, so  $\angle ADC = \phi'$  satisfies  $\phi + \phi' = \pi$ . The parallelogram case corresponds to the circle  $xx'yy'$  in Figure 29, with  $H$  at  $(\phi, \phi') = (\pi, 0)$  and  $G$  at  $(\phi, \phi') = (0, \pi)$ . The degenerate case with

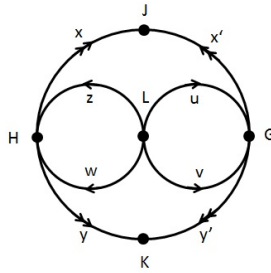


FIGURE 29. Configuration space for the rhombus

$\phi' = 0$  corresponds to the circle  $zw$ , with  $L$  at  $(\phi, \phi') = (0, 0)$ , while the case  $\phi = 0$  corresponds to the circle  $uv$ .

The reflection  $T$  takes  $(\phi, \phi')$  to  $(-\phi', -\phi)$ , while the rotation  $R$  takes  $(\phi, \phi')$  to  $(\phi', \phi)$ , unless  $\phi' = 0$  in which case  $(\phi, 0) \mapsto (0, -\phi)$ . Note that the two rules are consistent at  $H$  and  $L$ .  $\square$

### References

[BGRT] I. Basabe, J. González, Y.B. Rudyak, D. Tamaki, “Higher topological complexity and its symmetrization”, *Alg. Geom. Topology* **14** (2014), pp. 2103-2124.

[BR] A. Bianchi & D. Recio-Mitter, “Topological complexity of unordered configuration spaces of surfaces”, *Alg. Geom. Topology* **19** (2019), pp. 1359-1384.

[BS1] D. Blanc & N. Shvalb, “Generic singular configurations of linkages”, *Top. & Applic.* **159** (2012), pp. 877-890.

[BS2] D. Blanc & N. Shvalb, “Configuration spaces of spatial linkages: Taking Collisions Into Account”, *Bull. Kor. Math. Soc.* **54** (2017), pp. 2183-2210.

[BK] Z. Błaszczuk & M. Kaluba, “Effective topological complexity of spaces with symmetries”, *Pub. Mat.* **62** (2018), pp. 55-74.

[C] D.C. Cohen, “Topological complexity of classical configuration spaces and related objects”, in *Topological complexity and related topics*, Contemp. Math. **702**, AMS, Providence, RI, 2018, pp. 41-60.

[CDR] R. Connelly, E.D. Demaine, & G. Rote, “Straightening polygonal arcs and convexifying polygonal cycles”, *Discrete Comput. Geom.* **30** (2003), pp. 205-239.

[D] D.M. Davis, “Topological complexity of some planar polygon spaces”, *Bol. Soc. Mat. Mex. (3)* **23** (2017), pp. 129-139.

[FH] E.R. Fadell & S.Y. Husseini, *Geometry and topology of configuration spaces*,

[FN] E.R. Fadell & L.P. Neuwirth, “Configuration spaces”, *Math. Scand.* **10** (1962), pp. 111-118

[F1] M.S. Farber, “Topological complexity of motion planning”, *Discrete Comput. Geom.* **29** (2003), pp. 211-221.

[F2] M.S. Farber, *Invitation to Topological Robotics*, European Mathematical Society, Zurich, 2008.

[FG] M.S. Farber & M. Grant, “Symmetric Motion Planning”, in *Topology and robotics (Zurich, 2006)*, Contemp. Math. **438**, AMS, Providence, RI, 2007, pp. 85-104.

[FP] A. Franc & P. Pavešić, “Spaces with high topological complexity”, *Proc. Roy. Soc. Edin., Sec. A* **144** (2014), pp. 761-773.

- [GP] P. Galashin & G.Yu. Panina, “Manifolds associated to simple games”, *J. Knot Theory Ramif.* **25** (2016), No. 12.
- [G] R. Ghrist, “Configuration spaces, braids, and robotics”, in *Braids*, World Sci. Publ., Hackensack, NJ, 2010, pp. 263-304.
- [Hal] A.S. Hall, Jr., *Kinematics and linkage design*, Prentice-Hall, Englewood Cliffs, NJ, 1961.
- [HR] J.-C. Hausmann & E. Rodriguez, “The space of clouds in Euclidean space”, *Experiment. Math.* **13** (2004), pp. 31-47.
- [Hav] T.F. Havel, “Some examples of the use of distances as coordinates for Euclidean geometry”, *J. Symbolic Comput.* **11** (1991), pp. 579-593.
- [Hi] H. Hironaka, “Triangulations of algebraic sets”, in *Algebraic geometry (Humboldt State Univ., Arcata, Calif., 1974)*, Proc. Sympos. Pure Math. **29**, AMS, Providence, R.I., 1975, pp. 165-185.
- [HS] C. Housecroft & A.G. Sharpe, *Inorganic Chemistry*, 5th edition, Pearson International, London, UK, 2018.
- [K] Y. Kamiyama, “Topology of equilateral polygon linkages”, *Top. Applic.* **68** (1996), pp. 13-31.
- [KTe] Y. Kamiyama & M. Tezuka, “Topology and geometry of equilateral polygon linkages in the Euclidean plane”, *Quart. J. Math. Oxford (2)* **50** (1999), pp. 463-470.
- [KTs] Y. Kamiyama & S. Tsukuda, “The configuration space of the  $n$ -arms machine in the Euclidean space”, *Top. & Applic.* **154** (2007), pp. 1447-1464.
- [KM] M. Kapovich & J. Millson, “On Moduli Space of Polygons in the Euclidean Plane”, *J. Diff. Geom.* **42** (1995), pp. 430-464.
- [LLL] Fengling Li, Hao Li, & Zhi Lü, “A theory of orbit braids”, preprint, 2019 [arXiv:1903.11501](https://arxiv.org/abs/1903.11501).
- [L] S. Lojasiewicz, “Triangulation of semi-analytic sets”, *Ann. Scuola Norm. Sup. Pisa Cl. Sci. (3)* **18** (1964), pp. 449-474.
- [Ma] J.P. May, *Equivariant homotopy and cohomology theory*, American Mathematical Society, Providence, RI, 1996.
- [Me] J. P. Merlet, *Parallel Robots*, Kluwer Academic Publishers, Dordrecht, 2000.
- [MT] R.J. Milgram & J. C. Trinkle, “The Geometry of Configuration Spaces for Closed Chains in Two and Three Dimensions”, *Homology, Homotopy & Applic.* **6** (2004), pp. 237-267.
- [MW] A. Murillo-Mas & J. Wu, “Topological complexity of the work map”, *J. Top. Applic.* **12** (2021), pp. 219-238.
- [P] G.Yu. Panina, “Moduli space of planar polygonal linkage: a combinatorial description”, *Arnold Math. J.* **3** (2017), pp. 351-364.
- [S] J.M. Selig, *Geometric Fundamentals of Robotics*, Springer-Verlag *Mono. Comp. Sci.*, Berlin-New York, 2005.
- [SSBB] N. Shvalb, M. Shoham, H. Bamberger, & D. Blanc, “Topological and Kinematic Singularities for a Class of Parallel Mechanisms”, *Math. Prob. in Eng.* **2009** (2009), Art. 249349, pp. 1-12.
- [SSB] N. Shvalb, M. Shoham, & D. Blanc, “The Configuration Space of Arachnoid Mechanisms”, *Fund. Math.* **17** (2005), pp. 1033-1042.
- [T] L. W. Tsai, *Robot Analysis - The mechanics of serial and parallel manipulators*, Wiley interscience Publication - John Wiley & Sons, New York, 1999.

DAVID BLANC  
DEPARTMENT OF MATHEMATICS  
HAIFA UNIVERSITY  
HAIFA 3498838, ISRAEL  
*Email address:* `blanc@math.haifa.ac.il`

NIR SHVALB  
DEPARTMENT OF MECHANICAL ENGINEERING  
ARIEL UNIVERSITY  
ARIEL 40700, ISRAEL  
*Email address:* `nirsh@ariel.ac.il`